Disputation inom Teknisk mekanik

Lärosäte: Kungliga Tekniska Högskolan, Inst. Mekanik

Titel: **Transition delay in boundary-layer flows via reactive control**

Respondent: **Nicolò Fabbiane**

- Huvudhandledare: Prof. Dan S. Henningson, KTH Mekanik
- Biträdande handledare: Dr. Shervin Bagheri, KTH Mekanik
- Finansiär: VR 2012-4246

Opponent: **Dr. Denis Sipp**, ONERA DAFE, Frankrike

Betygsnämnden: Dr. Ati Sharma, University of Southampton, Storbritannien
Dr. Taraneh Sayadi, RWTH Aachen, Tyskland
Prof. Håkan Hjalmarsson, KTH Reglerteknik

Ordförande: Dr. Ardeshir Hanifi, FOI/KTH Mekanik

Disputationsakten:

1. Presentation av respondenten (ca 40 min).
2. Opponenten diskuterar och ställer frågor på avhandlingen.
3. Betygsnämnden ställer frågor.
4. Öppet för allmänheten att ställa frågor.

Public defense:

1. Presentation by the respondent (ca 40 min).
2. The opponent discusses the thesis with the respondent.
3. The members of the grading committee discuss the thesis with the respondent.
4. The audience is allowed and invited to ask questions.

Public defense:

1. Presentation by the respondent (ca 40 min).
2. The opponent discusses the thesis with the respondent.
3. The members of the grading committee discuss the thesis with the respondent.
4. The audience is allowed and invited to ask questions.

The procedure continues as follows:

1. The grading committee will deliberate behind locked doors and make a decision.
2. The decision will be announced by the committee at Mechanics department, Osquars Backe 18, 6th floor.
3. Lunch will be served for all the involved people, including registered participating audience.

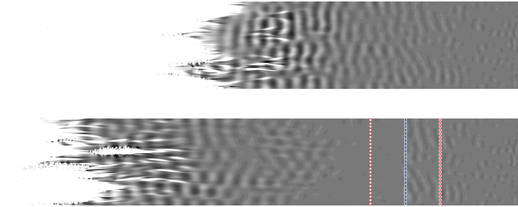

Transition delay in boundary-layer flows via reactive control

Nicolò Fabbiane

Linné FLOW Centre, KTH Mechanics, Stockholm

The project

Transition delay in boundary-layer flows

The project

Transition delay in boundary-layer flows

The project

Transition delay in boundary-layer flows

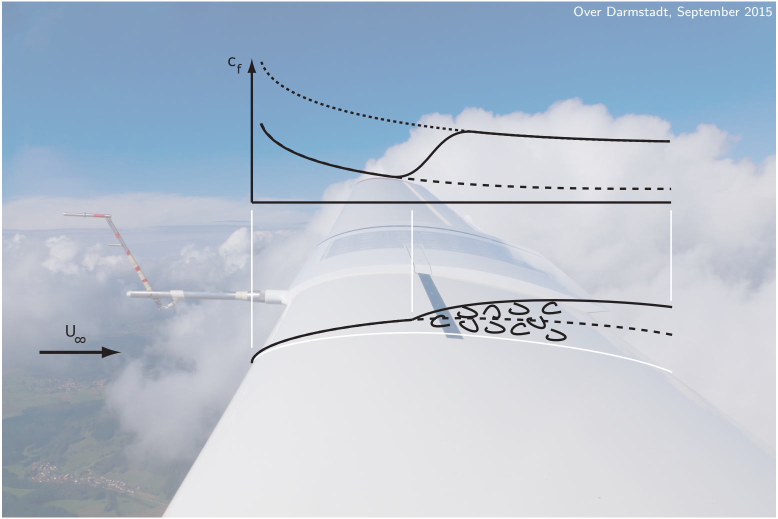

The project

Transition delay in boundary-layer flows

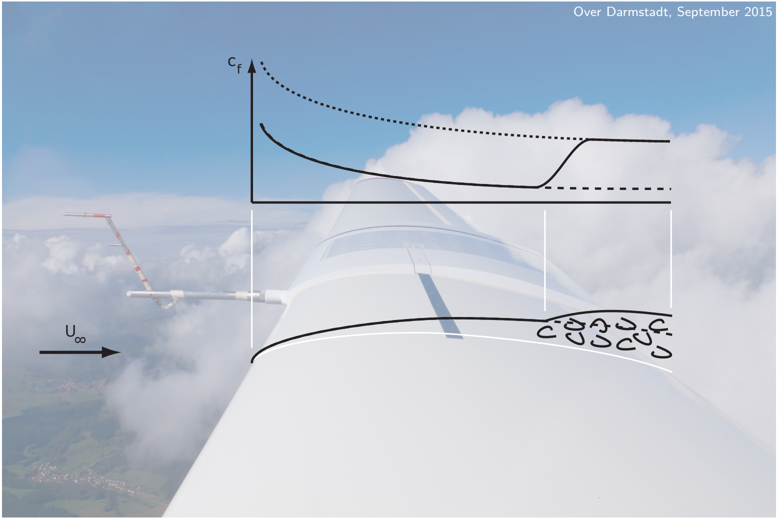

Routes to turbulence

Morkovin et al. (1994)

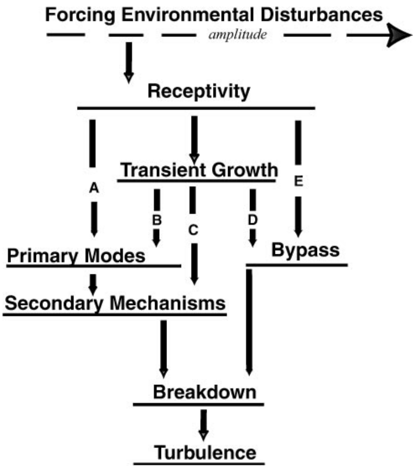

Routes to turbulence

Morkovin et al. (1994)

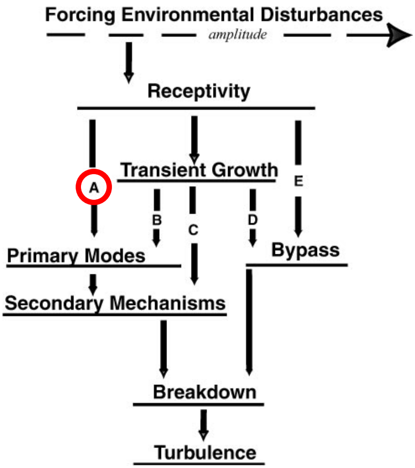

Routes to turbulence

Skin-friction fluctuations (grey-scale) and turbulent structures (green isosurfaces: λ_2-criterion)

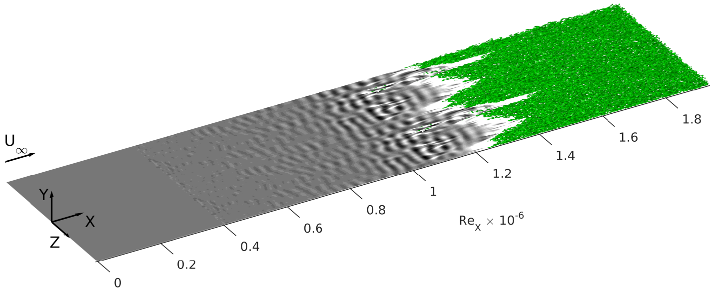

Routes to turbulence

Skin-friction fluctuations (grey-scale) and turbulent structures (green isosurfaces: λ_2-criterion)

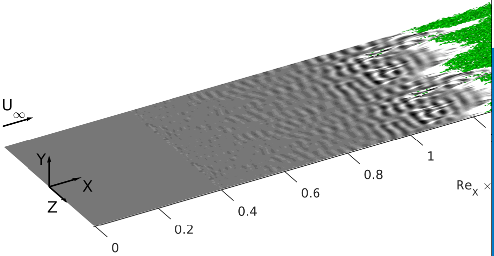

Pseudo-spectral DNS/LES code (SIMSON)

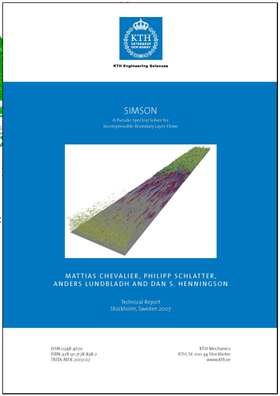

Chevalier et al. (2007)

The control strategy

Attenuation of Tollmien-Schlichting (TS) instabilities

The control strategy

Attenuation of Tollmien-Schlichting (TS) instabilities

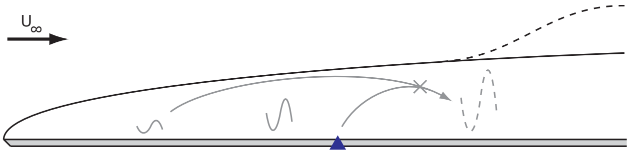

The control strategy

Attenuation of Tollmien-Schlichting (TS) instabilities

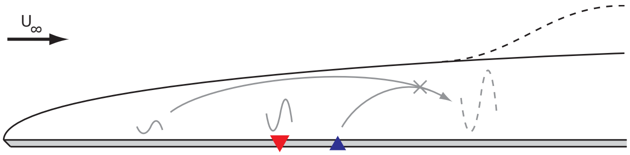

The control strategy

Attenuation of Tollmien-Schlichting (TS) instabilities

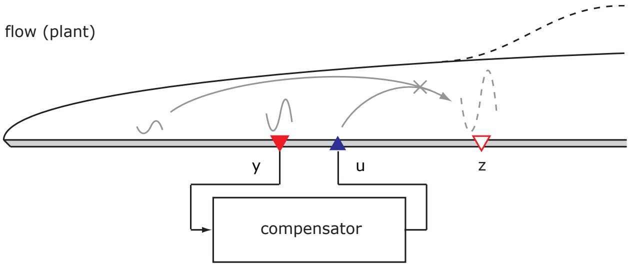

The reactive control problem

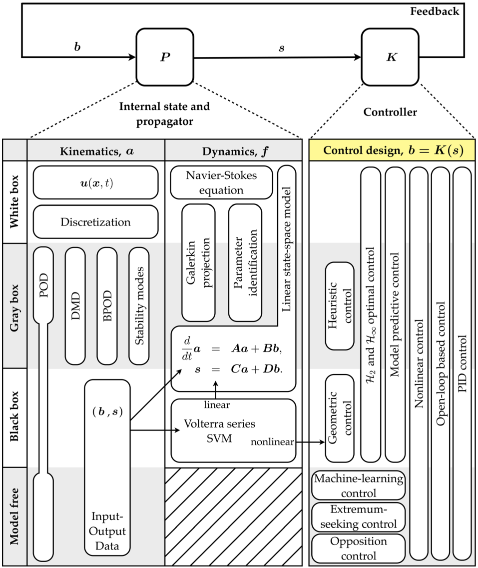

Brunton and Noack (2015)

The reactive control problem

Bewley and Liu (1998)

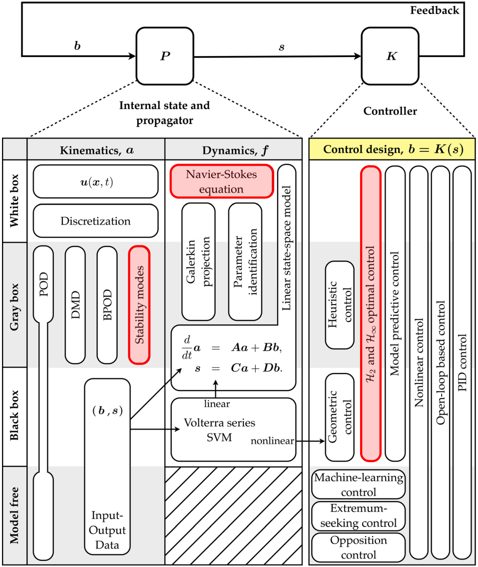

Brunton and Noack (2015)

The reactive control problem

Bewley and Liu (1998)

Sturzebecher and Nitsche (2003)

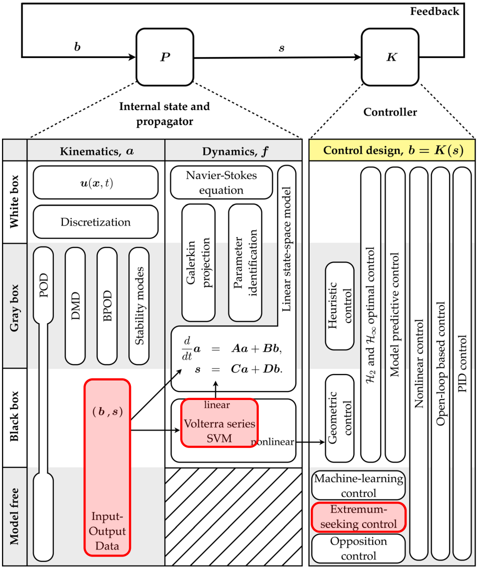

Brunton and Noack (2015)

The reactive control problem

Bewley and Liu (1998)

Sturzebecher and Nitsche (2003)

Li and Gaster (2006)

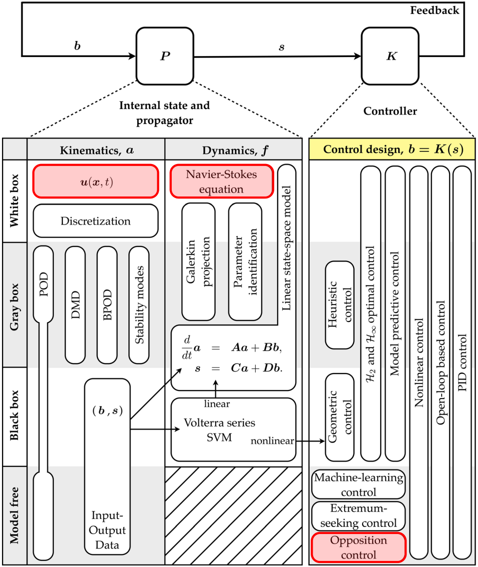

Brunton and Noack (2015)

The reactive control problem

- Bewley and Liu (1998)
- Sturzebecher and Nitsche (2003)
- Li and Gaster (2006)
- Bagheri et al. (2009)

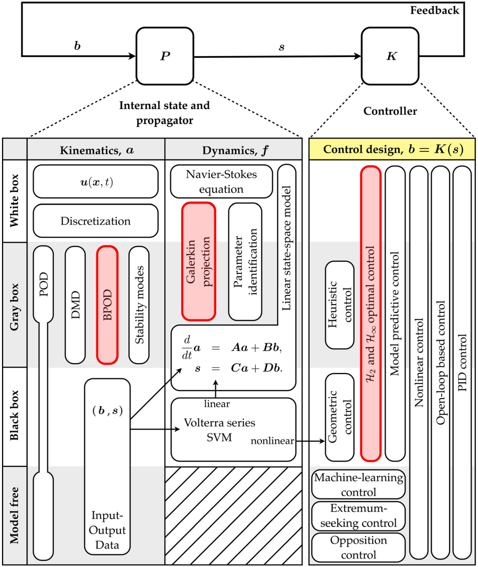

Brunton and Noack (2015)

The reactive control problem

Bewley and Liu (1998)

Sturzebecher and Nitsche (2003)

Li and Gaster (2006)

Barbagallo et al. (2009)
Bagheri et al. (2009)

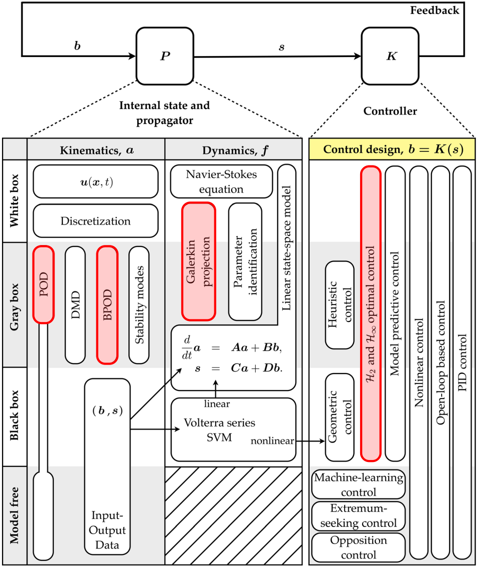

Brunton and Noack (2015)

The reactive control problem

Bewley and Liu (1998)

Sturzebecher and Nitsche (2003)

Li and Gaster (2006)

Barbagallo et al. (2009)

Bagheri et al. (2009)

Sharma et al. (2011)

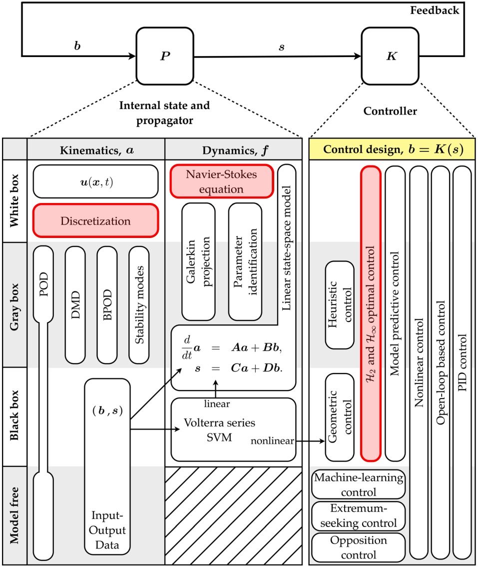

Brunton and Noack (2015)

The reactive control problem

Bewley and Liu (1998)

Sturzebecher and Nitsche (2003)

Li and Gaster (2006)

Barbagallo et al. (2009)

Bagheri et al. (2009)

Sharma et al. (2011)

Kurz et al. (2013)

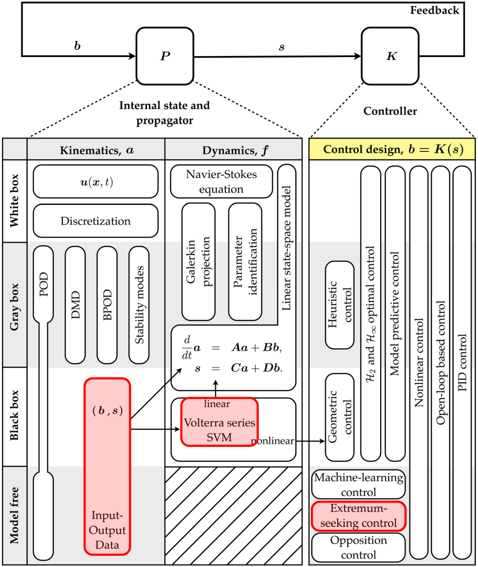

Brunton and Noack (2015)

The reactive control problem

- Bewley and Liu (1998)
- Sturzebecher and Nitsche (2003)
- Li and Gaster (2006)
- Barbagallo et al. (2009)
- Bagheri et al. (2009)
- Sharma et al. (2011)
- Semeraro et al. (2013)
- Kurz et al. (2013)

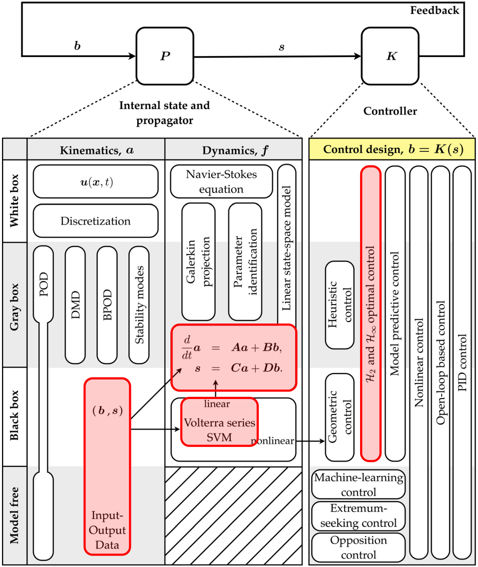

Brunton and Noack (2015)

The reactive control problem

- Bewley and Liu (1998)
- Sturzebecher and Nitsche (2003)
- Li and Gaster (2006)
- Barbagallo et al. (2009)
- Bagheri et al. (2009)
- Sharma et al. (2011)
- Semeraro et al. (2013)
- Kurz et al. (2013)
- Juillet et al. (2014)

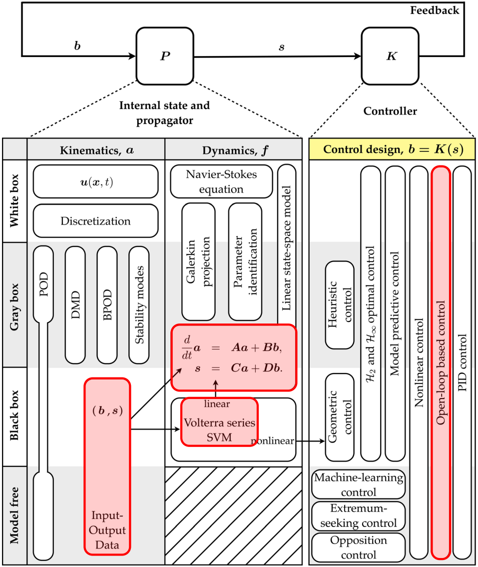

Brunton and Noack (2015)

The reactive control problem

- Bewley and Liu (1998)
- Sturzebecher and Nitsche (2003)
- Li and Gaster (2006)
- Barbagallo et al. (2009)
- Bagheri et al. (2009)
- Sharma et al. (2011)
- Semeraro et al. (2013)
- Kurz et al. (2013)
- Juillet et al. (2014)
- Kotsonis et al. (2015)

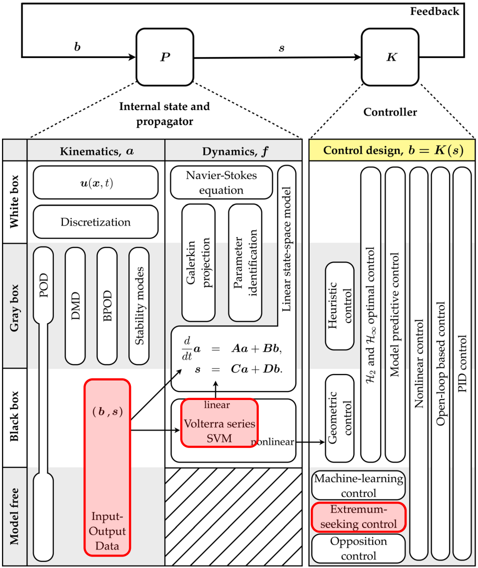

Brunton and Noack (2015)

The reactive control problem

- Bewley and Liu (1998)
- Sturzebecher and Nitsche (2003)
- Li and Gaster (2006)
- Barbagallo et al. (2009)
- Bagheri et al. (2009)
- Sharma et al. (2011)
- Semeraro et al. (2013)
- Kurz et al. (2013)
- Juillet et al. (2014)
- Kotsonis et al. (2015)

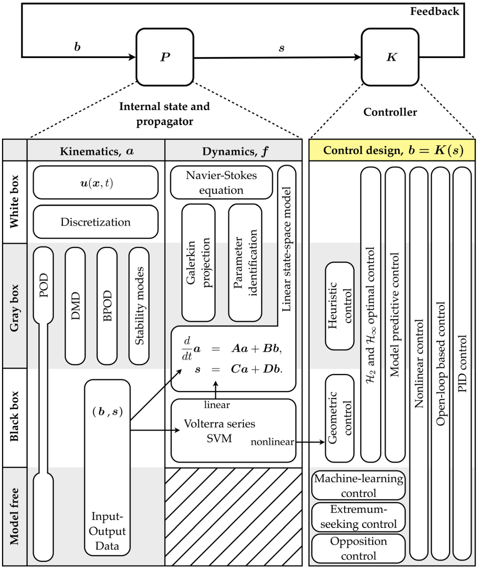

Brunton and Noack (2015)

The reactive control problem

Bewley and Liu (1998)

Sturzebecher and Nitsche (2003)

Li and Gaster (2006)

Barbagallo et al. (2009)
Bagheri et al. (2009)

Sharma et al. (2011)
Semeraro et al. (2013)
Kurz et al. (2013)
Juillet et al. (2014)
Kotsonis et al. (2015)

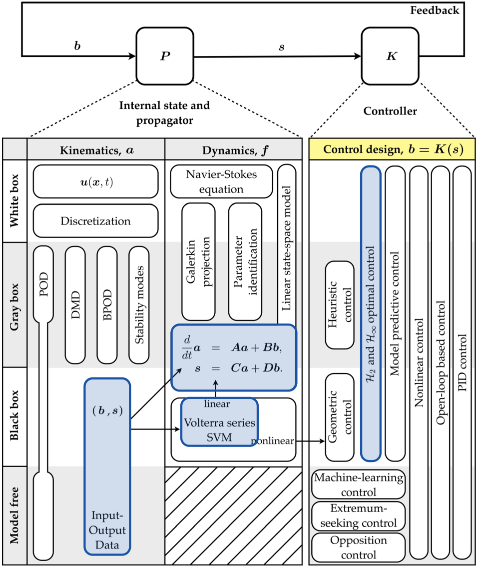

Brunton and Noack (2015)

The reactive control problem

Bewley and Liu (1998)

Sturzebecher and Nitsche (2003)

Li and Gaster (2006)

Barbagallo et al. (2009)

Bagheri et al. (2009)

Sharma et al. (2011)

Semeraro et al. (2013)

Kurz et al. (2013)

Juillet et al. (2014)

Kotsonis et al. (2015)

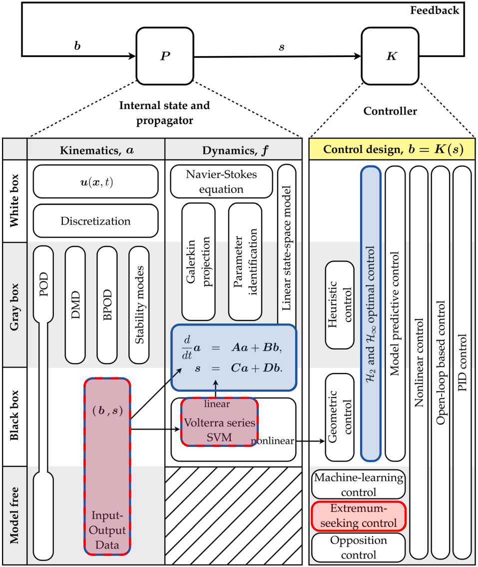

Brunton and Noack (2015)

The reactive control problem

Bewley and Liu (1998)

Sturzebecher and Nitsche (2003)

Li and Gaster (2006)

Barbagallo et al. (2009)

Bagheri et al. (2009)

Sharma et al. (2011)

Semeraro et al. (2013)

Kurz et al. (2013)

Juillet et al. (2014)

Kotsonis et al. (2015)

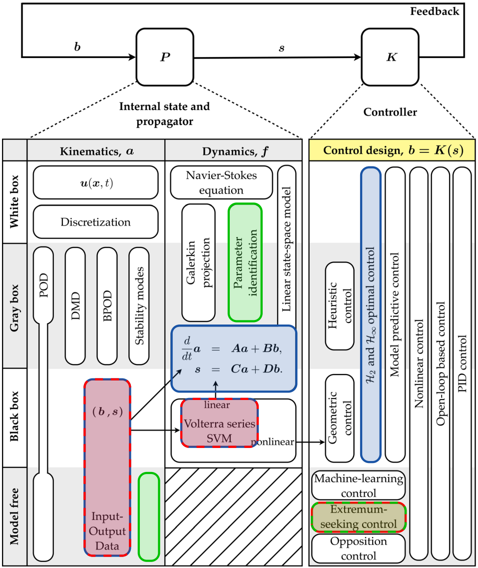

Brunton and Noack (2015)

Outline

Control of boundary-layer instabilities
- A linear model of the flow
- Control algorithms
- A self-tuning compensator

Transition delay
- A 3D compensator
- Performance and limitations
- Energy budget

Conclusions and Outlook

Outline

Control of boundary-layer instabilities
- A linear model of the flow
- Control algorithms
- A self-tuning compensator

Transition delay
- A 3D compensator
- Performance and limitations
- Energy budget

Conclusions and Outlook

Plant response

Impulse response by the disturbance d

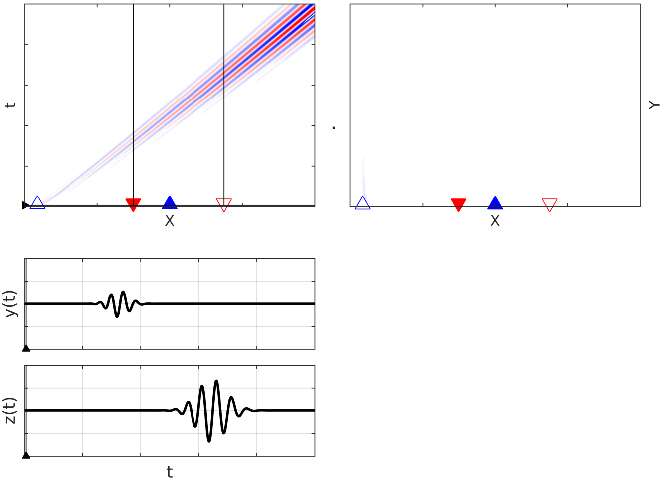

Plant response

Impulse response by the disturbance d

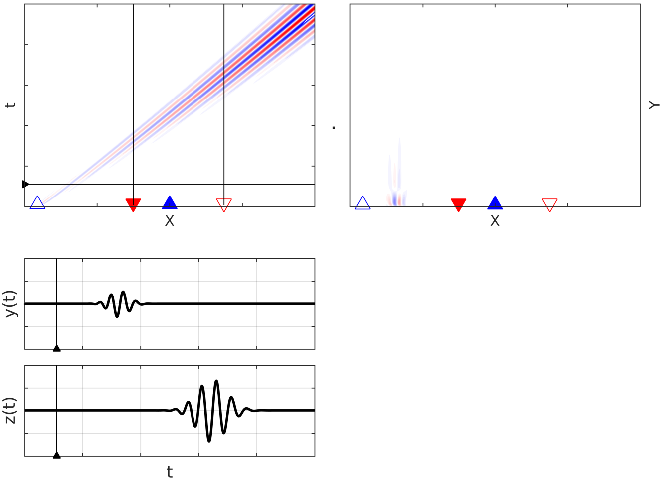

Plant response

Impulse response by the disturbance d

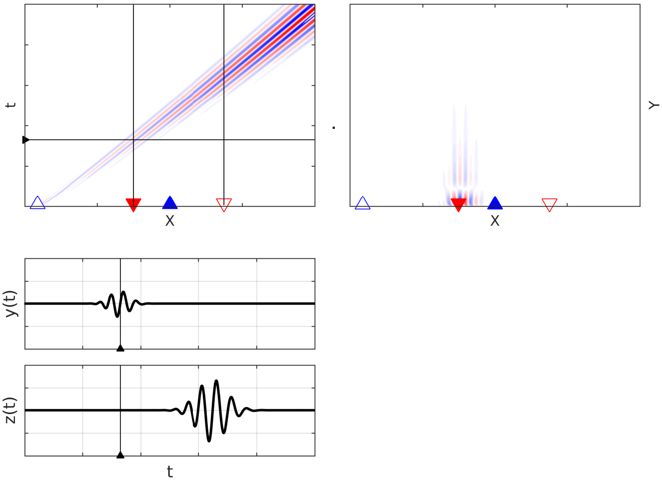

Plant response

Impulse response by the disturbance d

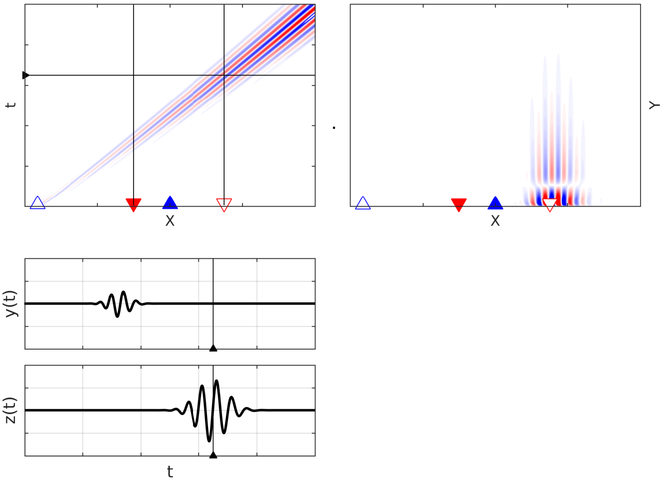

Plant response

Impulse response by the disturbance d

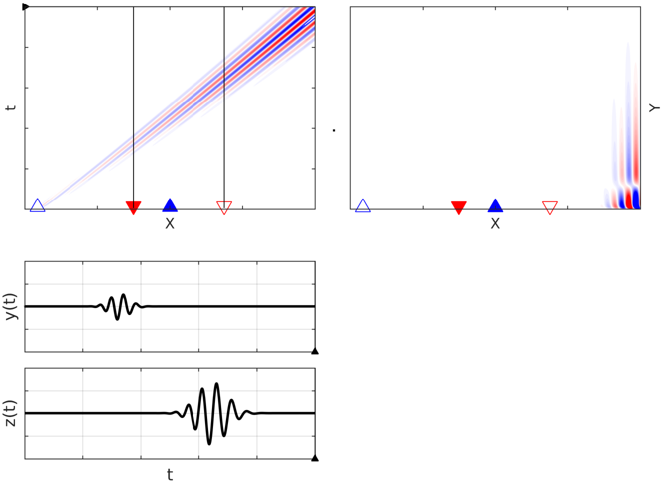

Plant response

Impulse response by the actuator u

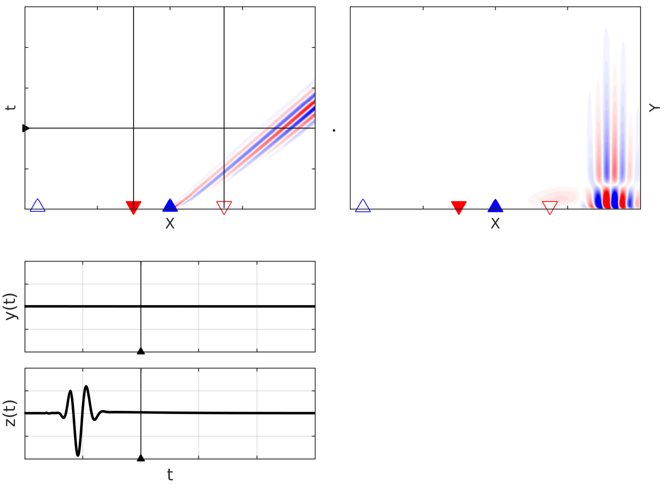

Plant response

Impulse response by the actuator u

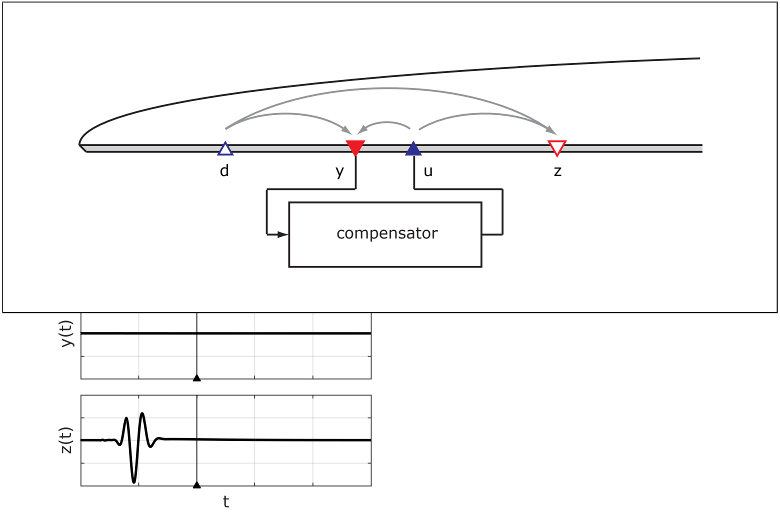

Plant response

Impulse response by the actuator u

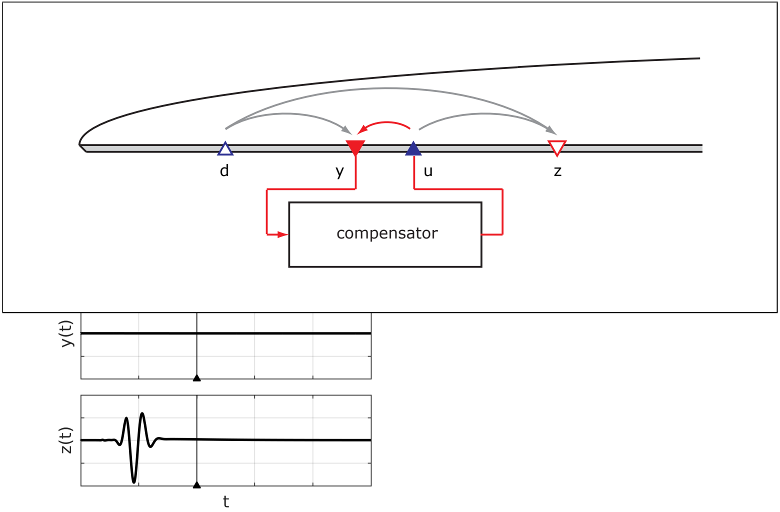

Plant response

Impulse response by the actuator u

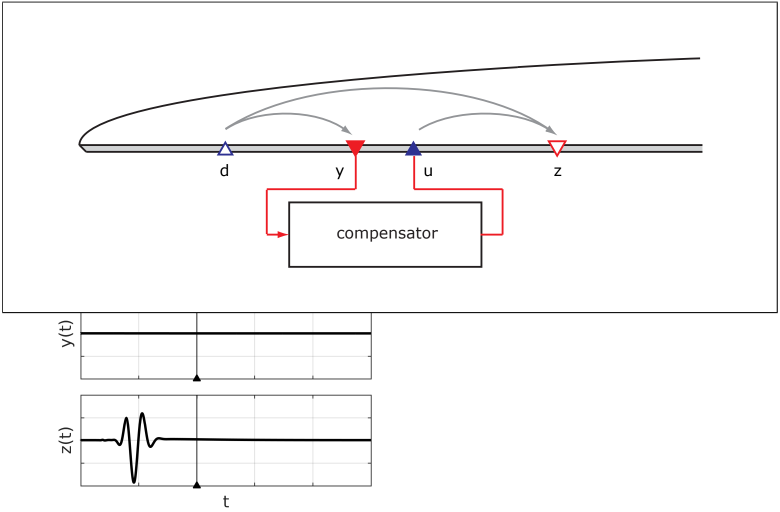

Plant response

Impulse response by the actuator u

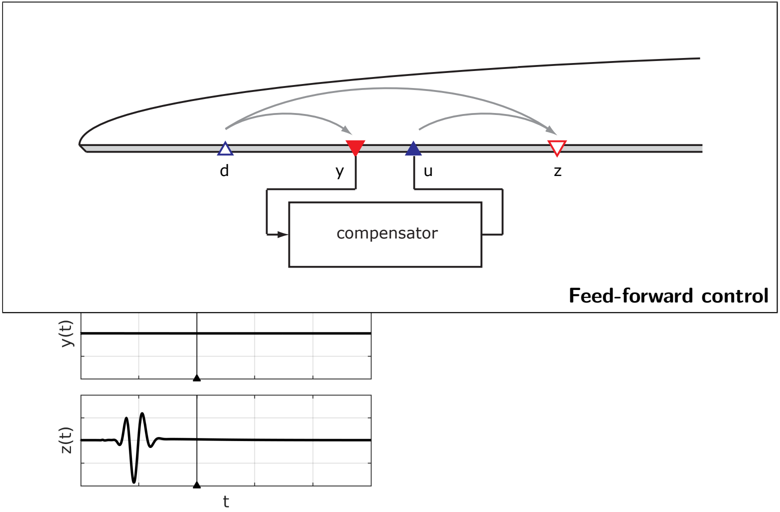

Linear state-space model

2D linear perturbation of a 2D boundary-layer flow over a flat plate

Linearised Navier-Stokes (LNS) eq.s around the baseflow $\mathbf{U}(\mathbf{x})$:

$$\frac{\partial \mathbf{u}}{\partial t} = -(\mathbf{U}\cdot\nabla)\,\mathbf{u} - (\mathbf{u}\cdot\nabla)\,\mathbf{U} - \nabla p + \frac{1}{Re}\nabla^2\mathbf{u}$$
$$0 = \nabla\cdot\mathbf{u}$$

Linear state-space model

2D linear perturbation of a 2D boundary-layer flow over a flat plate

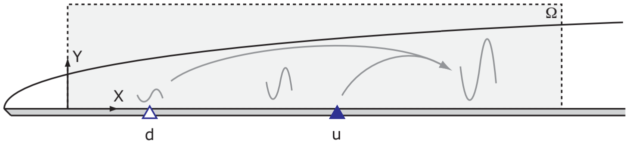

Linearised Navier-Stokes (LNS) eq.s around the baseflow $\mathbf{U}(\mathbf{x})$:

$$\frac{\partial \mathbf{u}}{\partial t} = -(\mathbf{U}\cdot\nabla)\,\mathbf{u} - (\mathbf{u}\cdot\nabla)\,\mathbf{U} - \nabla p + \frac{1}{Re}\nabla^2\mathbf{u} \;+\; \mathbf{b}_d(\mathbf{x})\,d(t) + \mathbf{b}_u(\mathbf{x})\,u(t)$$
$$0 = \nabla\cdot\mathbf{u}$$

Linear state-space model

2D linear perturbation of a 2D boundary-layer flow over a flat plate

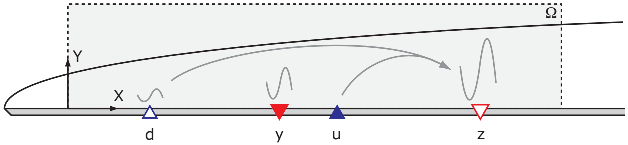

Linearised Navier-Stokes (LNS) eq.s around the baseflow $\mathbf{U}(\mathbf{x})$:

$$\frac{\partial \mathbf{u}}{\partial t} = -(\mathbf{U}\cdot\nabla)\,\mathbf{u} - (\mathbf{u}\cdot\nabla)\,\mathbf{U} - \nabla p + \frac{1}{Re}\nabla^2\mathbf{u} \; + \; \mathbf{b}_d(\mathbf{x})\, d(t) + \mathbf{b}_u(\mathbf{x})\, u(t)$$

$$0 = \nabla\cdot\mathbf{u}$$

$$y(t) = \int_\Omega \mathbf{c}_y(\mathbf{x})\cdot\mathbf{u}(\mathbf{x},t)\, d\Omega$$

$$z(t) = \int_\Omega \mathbf{c}_z(\mathbf{x})\cdot\mathbf{u}(\mathbf{x},t)\, d\Omega$$

Linear state-space model

2D linear perturbation of a 2D boundary-layer flow over a flat plate

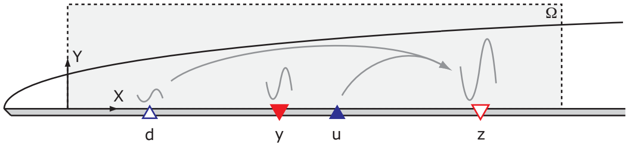

Linearised Navier-Stokes (LNS) eq.s around the baseflow $\mathbf{U}(\mathbf{x})$:

$$\dot{\mathbf{q}}(t) = \mathbf{A}\;\mathbf{q}(t) + \mathbf{B}_d\, d(t) + \mathbf{B}_u\, u(t)$$

$$y(t) = \mathbf{C}_y\, \mathbf{q}(t)$$

$$z(t) = \mathbf{C}_z\, \mathbf{q}(t)$$

where $\mathbf{u}(\mathbf{x}, t) \approx \mathbf{T}(\mathbf{x})\, \mathbf{q}(t)$.

Linear Quadratic Gaussian (LQG) regulator

$$\dot{\mathbf{q}}(t) = \mathbf{A}\ \mathbf{q}(t) + \mathbf{B}_d\, d(t) + \mathbf{B}_u\, u(t)$$

$$y(t) = \mathbf{C}_y\, \mathbf{q}(t)$$

$$z(t) = \mathbf{C}_z\, \mathbf{q}(t)$$

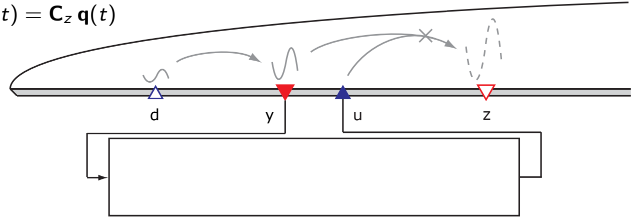

Linear Quadratic Gaussian (LQG) regulator

$\dot{\mathbf{q}}(t) = \mathbf{A}\ \mathbf{q}(t) + \mathbf{B}_d\, d(t) + \mathbf{B}_u\, u(t)$

$y(t) = \mathbf{C}_y\, \mathbf{q}(t)$

$z(t) = \mathbf{C}_z\, \mathbf{q}(t)$

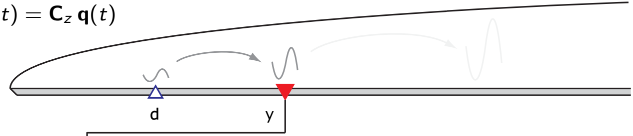

$\dot{\hat{\mathbf{q}}}(t) = (\mathbf{A} + \mathbf{L}\mathbf{C}_y)\, \hat{\mathbf{q}}(t) - \mathbf{L}\, y(t)$

Observer: Kalman filter

$$\min \left[\lim_{T\to\infty} \frac{1}{T} \int_0^T \|\mathbf{q}(t) - \hat{\mathbf{q}}(t)\|_2^2 \ dt \right]$$

Under a stochastic forcing $d(t)$ and $n(t)$,

$$\boxed{\mathbf{L} = -\mathbf{Y}\mathbf{C}_y^H R_n^{-1},}$$

where $\mathbf{Y}$ is solution to the Riccati eq.:

$$\mathbf{AY} + \mathbf{YA}^H - \mathbf{Y}\,\mathbf{C}_y{}^H R_n^{-1} \mathbf{C}_y\,\mathbf{Y} + \mathbf{B}_d R_d \mathbf{B}_d{}^H = \mathbf{0}$$

Linear Quadratic Gaussian (LQG) regulator

$\dot{\mathbf{q}}(t) = \mathbf{A}\ \mathbf{q}(t) + \mathbf{B}_d\, d(t) + \mathbf{B}_u\, u(t)$

$y(t) = \mathbf{C}_y\, \mathbf{q}(t)$

$z(t) = \mathbf{C}_z\, \mathbf{q}(t)$

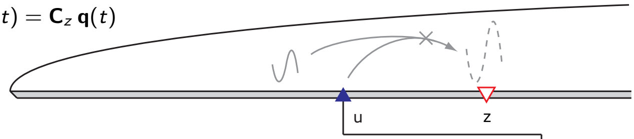

$\dot{\hat{\mathbf{q}}}(t) = (\mathbf{A} \qquad)\, \hat{\mathbf{q}}(t) \qquad + \mathbf{B}_u\, u(t)$

$u(t) = \mathbf{K}\hat{\mathbf{q}}(t)$

Controller: LQR

$$\min \left[\int_0^\infty \left(w_z z^2(t) + w_u\, u^2(t) \right)\, dt \right]$$

The control gain matrix is obtained as

$$\boxed{\mathbf{K} = -w_u^{-1}\mathbf{B}_u\mathbf{X},}$$

where $\mathbf{X}$ is solution to the Riccati eq.:

$$\mathbf{A}^H\mathbf{X} + \mathbf{X}\mathbf{A} - \mathbf{X}\,\mathbf{B}_u\ w_u^{-1}\mathbf{B}_u{}^H\,\mathbf{X} + \mathbf{C}_z{}^H w_z\mathbf{C}_z = \mathbf{0}.$$

Linear Quadratic Gaussian (LQG) regulator

$$\dot{\mathbf{q}}(t) = \mathbf{A}\;\mathbf{q}(t) + \mathbf{B}_d\, d(t) + \mathbf{B}_u\, u(t)$$

$$y(t) = \mathbf{C}_y\, \mathbf{q}(t)$$

$$z(t) = \mathbf{C}_z\, \mathbf{q}(t)$$

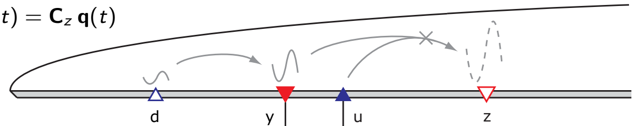

$$\boxed{\begin{aligned} \dot{\hat{\mathbf{q}}}(t) &= (\mathbf{A} + \mathbf{L}\mathbf{C}_y)\,\hat{\mathbf{q}}(t) - \mathbf{L}\, y(t) + \mathbf{B}_u\, u(t) \\ u(t) &= \mathbf{K}\hat{\mathbf{q}}(t) \end{aligned}}$$

Observer: Kalman filter

$$\min \left[\lim_{T\to\infty} \frac{1}{T} \int_0^T \|\mathbf{q}(t) - \hat{\mathbf{q}}(t)\|_2^2 \;dt \right]$$

Under a stochastic forcing $d(t)$ and $n(t)$,

$$\boxed{\mathbf{L} = -\mathbf{Y}\mathbf{C}_y^H R_n^{-1},}$$

where $\mathbf{Y}$ is solution to the Riccati eq.:

$$\mathbf{AY} + \mathbf{YA}^H - \mathbf{Y}\,\mathbf{C}_y{}^H R_n^{-1} \mathbf{C}_y\,\mathbf{Y} + \mathbf{B}_d R_d \mathbf{B}_d{}^H = \mathbf{0}$$

Controller: LQR

$$\min \left[\int_0^\infty \left(w_z z^2(t) + w_u\, u^2(t) \right) \;dt \right]$$

The control gain matrix is obtained as

$$\boxed{\mathbf{K} = -w_u^{-1}\mathbf{B}_u\mathbf{X},}$$

where $\mathbf{X}$ is solution to the Riccati eq.:

$$\mathbf{A}^H\mathbf{X} + \mathbf{XA} - \mathbf{X}\,\mathbf{B}_u\;w_u^{-1}\mathbf{B}_u{}^H\,\mathbf{X} + \mathbf{C}_z{}^H w_z \mathbf{C}_z = \mathbf{0}.$$

Input/Output (I/O) representation

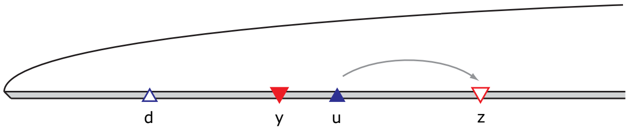

Forced response $z(t)$ by $u(t)$ with $\mathbf{q}_0 = \mathbf{0}$

$$z(t) = \mathbf{C}_z e^{\mathbf{A}t}\,\mathbf{q}_0 + \int_0^t \mathbf{C}_z e^{\mathbf{A}\tau}\mathbf{B}_u\, u(t-\tau)d\tau$$

Input/Output (I/O) representation

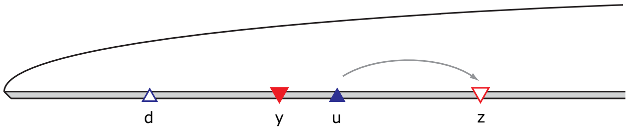

Forced response $z(t)$ by $u(t)$ with $\mathbf{q}_0 = \mathbf{0}$

$$z(t) = \int_0^t \mathbf{C}_z e^{\mathbf{A}\tau} \mathbf{B}_u \, u(t-\tau) d\tau$$

The 2×2 impulse responses represent the complete I/O properties of the plant.

Input/Output (I/O) representation

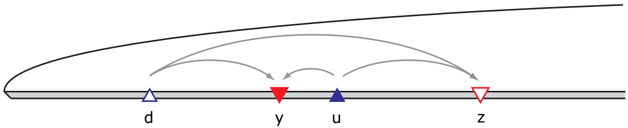

Forced response $y(t)$ and $z(t)$ by $d(t)$ and $u(t)$ with $\mathbf{q}_0 = \mathbf{0}$

$$y(t) = \int_0^t P_{yd}(\tau)\, d(t-\tau)d\tau + \int_0^t P_{yu}(\tau)\, u(t-\tau)d\tau$$

$$z(t) = \int_0^t P_{zd}(\tau)\, d(t-\tau)d\tau + \int_0^t P_{zu}(\tau)\, u(t-\tau)d\tau$$

The 2×2 impulse responses represent the complete I/O properties of the plant.

Input/Output (I/O) representation

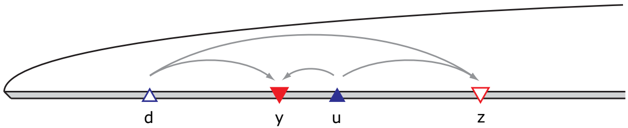

Forced response $y(t)$ and $z(t)$ by $d(t)$ and $u(t)$ with $\mathbf{q}_0 = \mathbf{0}$

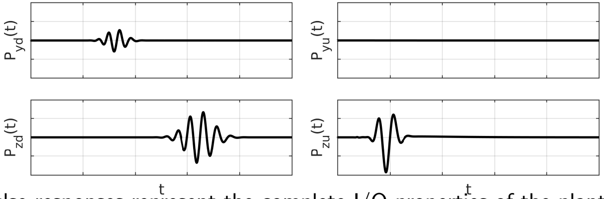

The 2×2 impulse responses represent the complete I/O properties of the plant.

Input/Output (I/O) representation

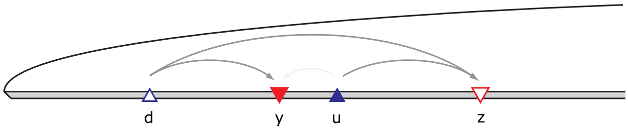

Forced response $y(t)$ and $z(t)$ by $d(t)$ and $u(t)$ with $\mathbf{q}_0 = \mathbf{0}$

$$y(t) \simeq \int_0^{T_{yd}} P_{yd}(\tau)\, d(t-\tau) d\tau$$

$$z(t) \simeq \int_0^{T_{zd}} P_{zd}(\tau)\, d(t-\tau) d\tau + \int_0^{T_{zu}} P_{zu}(\tau)\, u(t-\tau) d\tau$$

The 2×2 impulse responses represent the complete I/O properties of the plant.

Input/Output (I/O) representation

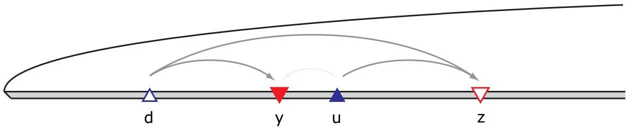

Forced response $y(n)$ and $z(n)$ by $d(n)$ and $u(n)$ with $\mathbf{q}_0 = \mathbf{0}$

$$y(n) \simeq \sum_{j=0}^{N_{yd}} P_{yd}(i)\, d(n-i)$$

$$z(n) \simeq \sum_{j=0}^{N_{zd}} P_{zd}(i)\, d(n-i) + \sum_{j=0}^{N_{zu}} P_{zu}(i)\, u(n-i)$$

Finite Impulse Response (FIR) filter

Filtered-X Least-Mean-Square (fxLMS) algorithm

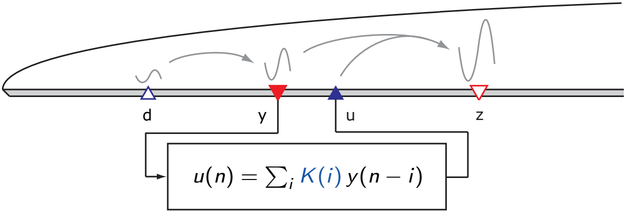

Filtered-X Least-Mean-Square (fxLMS) algorithm

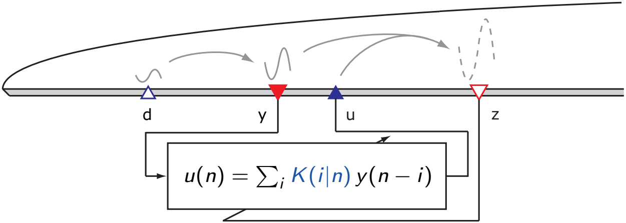

Minimise the cost function

$$\min_{K(i)} \left[z^2(n) \right]$$

via a steepest-descent algorithm

$$\boxed{K(i|n+1) = K(i|n) - \mu\, \lambda(i|n).}$$

with $\lambda(i|n) = \frac{\partial z^2}{\partial K(i)} = 2\, z(n) \sum_j P_{zu}(j)\; y(n-j) = 2\, z(n)\; f(n-i).$

Filtered-X Least-Mean-Square (fxLMS) algorithm

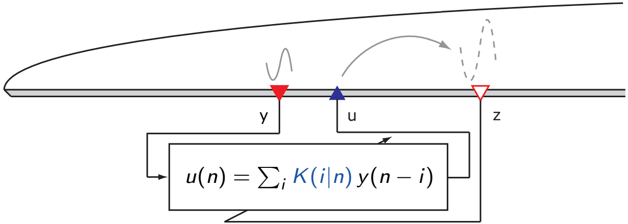

Minimise the cost function

$$\min_{K(i)} \left[z^2(n) \right]$$

via a steepest-descent algorithm

$$\boxed{K(i|n+1) = K(i|n) - \mu\, \lambda(i|n).}$$

with $\lambda(i|n) = \frac{\partial z^2}{\partial K(i)} = 2\, z(n) \sum_j P_{zu}(j)\; y(n-j) = 2\, z(n)\; f(n-i).$

Model-based vs. Adaptive control

Paper 1, Paper 2

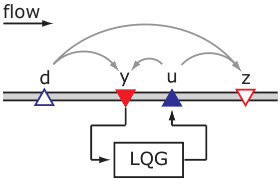

$$\dot{\hat{\mathbf{q}}}(t) = (\mathbf{A} + \mathbf{L}\mathbf{C}_y + \mathbf{B}_u\mathbf{K})\,\hat{\mathbf{q}}(t) - \mathbf{L}y(t)$$
$$u(t) = \mathbf{K}\hat{\mathbf{q}}(t)$$

- Based on a full model of the flow.
- Designed a-priori $\Rightarrow$ static.
- Optimal performances.
- Model reduction usually needed.

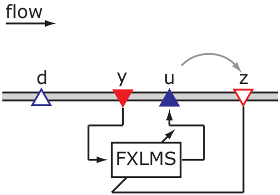

$$u(n) = \sum_i K(i|n)\, y(n-i)$$

- Only $u \rightarrow z$ needed.
- On-line minimisation $\Rightarrow$ adaptive.
- Reliable y-measurement.
- Measurable cost function.

Performance

Control of 2D linear perturbation in a 2D boundary-layer flow over a flat plate (Paper 2)

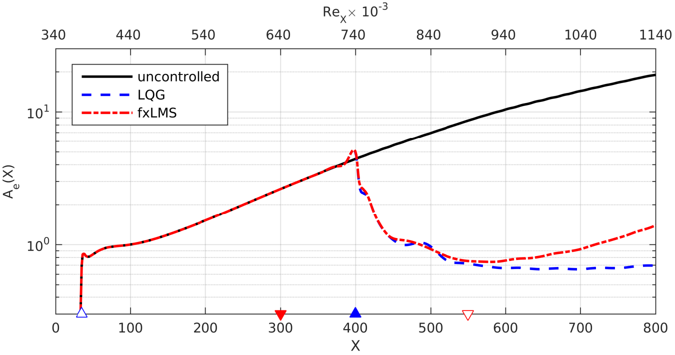

Performance and limitations

Control of 2D linear perturbation in a 2D boundary-layer flow over a flat plate (Paper 2)

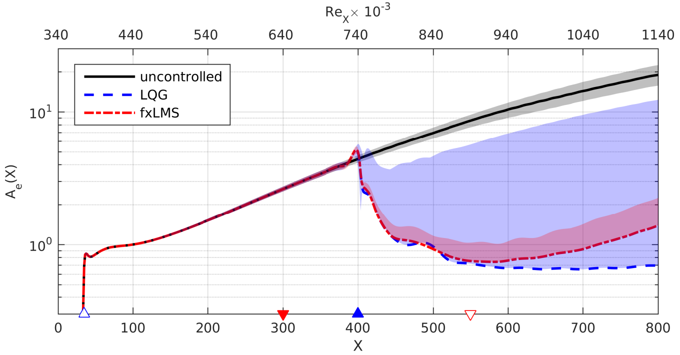

$\pm 5\%$ free-stream speed variations with respect to U_∞

Performance and limitations

Control of 2D linear perturbation in a 2D boundary-layer flow over a flat plate (Paper 2)

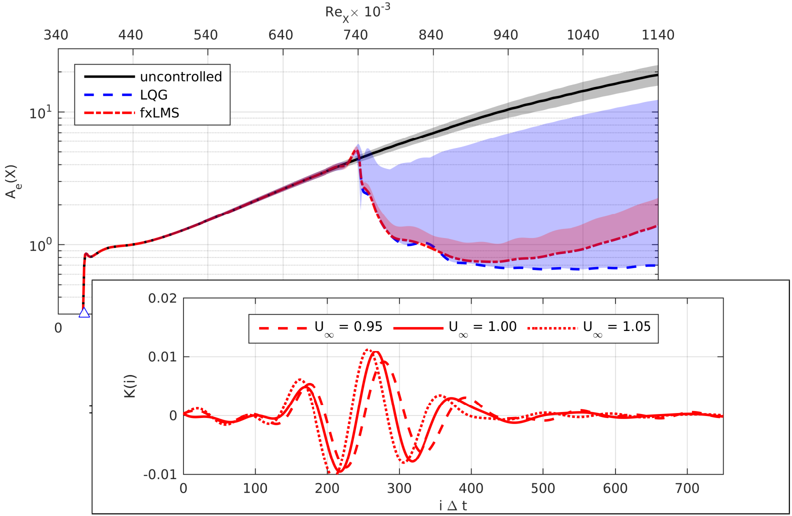

Performance and limitations

Control of 2D linear perturbation in a 2D boundary-layer flow over a flat plate (Paper 2)

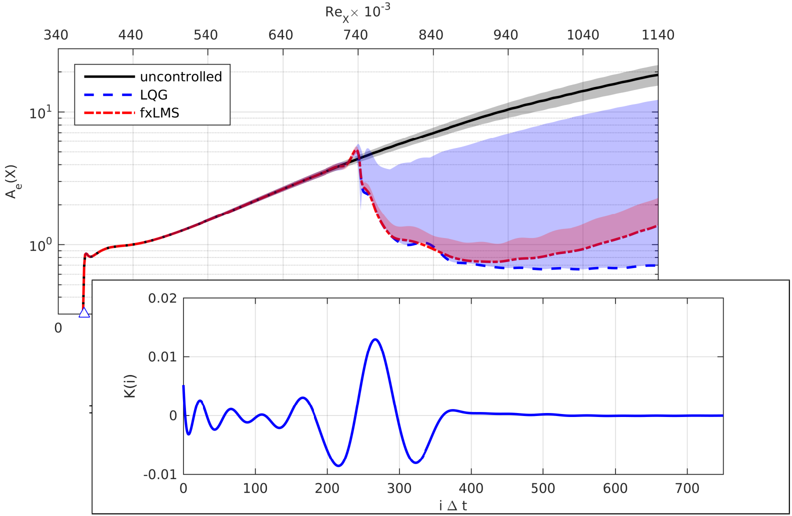

Performance and limitations

Control of 2D linear perturbation in a 2D boundary-layer flow over a flat plate (Paper 2)

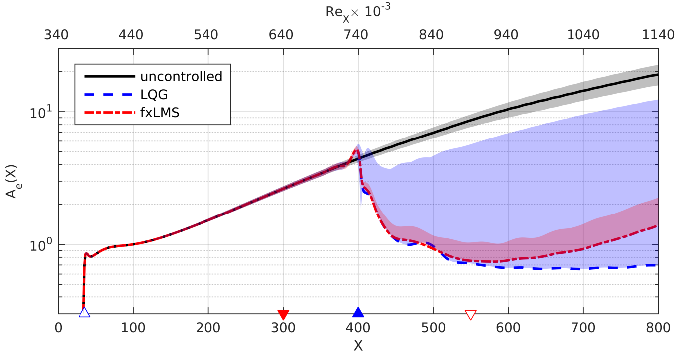

$\pm 5\%$ free-stream speed variations with respect to U_∞

Experimental setup

Open wind-tunnel @ TU Darmstadt (Paper 2)

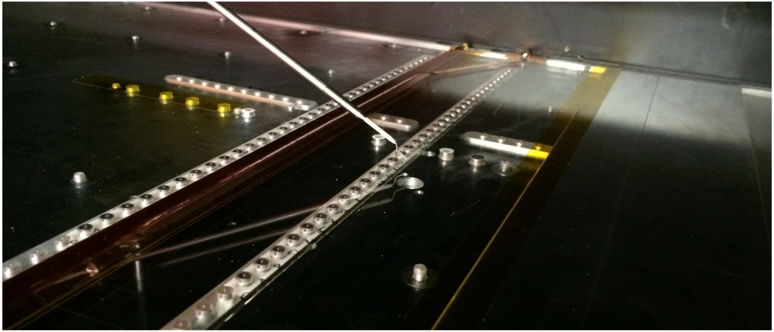

Disturbances: 15 independent loudspeakers producing 2D disturbances

Sensors: 2 surface hot-wires $\Rightarrow$ skin friction measurements

Actuator: 1 dielectric-barrier-discharge (DBD) plasma actuator $L = 230\,\text{mm}$

2 rows of 30 microphones each monitor the bi-dimensionality of the disturbances.

Experimental setup

Open wind-tunnel @ TU Darmstadt (Paper 2)

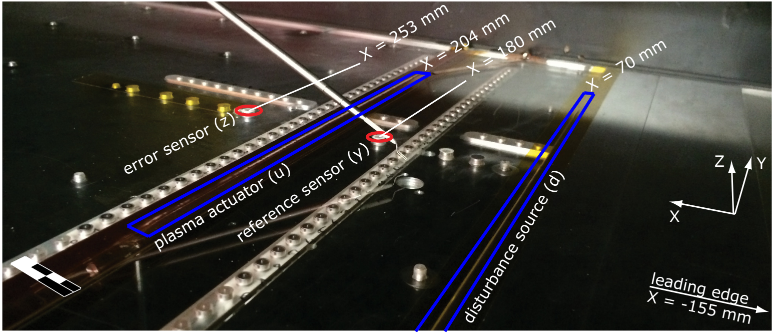

Disturbances:	15 independent loudspeakers producing 2D disturbances
Sensors:	2 surface hot-wires ⇒ skin friction measurements
Actuator:	1 dielectric-barrier-discharge (DBD) plasma actuator $L = 230\,\text{mm}$

2 rows of 30 microphones each monitor the bi-dimensionality of the disturbances.

Plasma actuator

- 2 copper electrodes separated by a dielectric material (Kapton tape)
- Plasma arch between the two electrodes

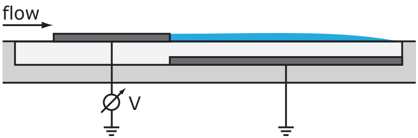

Plasma actuator

- 2 copper electrodes separated by a dielectric material (Kapton tape)
- Plasma arch between the two electrodes ⇒ force on the flow

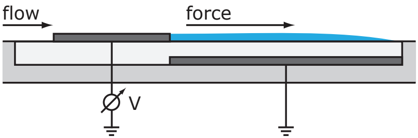

Plasma actuator

- 2 copper electrodes separated by a dielectric material (Kapton tape)
- Plasma arch between the two electrodes $\Rightarrow$ force on the flow

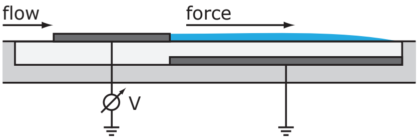

- Driven by the compensator via $u(t) \to V(t)$

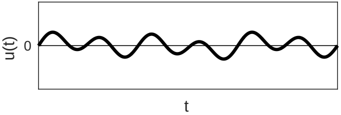

Plasma actuator

- 2 copper electrodes separated by a dielectric material (Kapton tape)
- Plasma arch between the two electrodes $\Rightarrow$ force on the flow

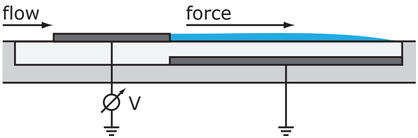

- Driven by the compensator via $u(t) \rightarrow V(t)$

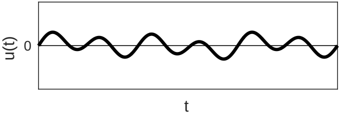

- Force in one direction only

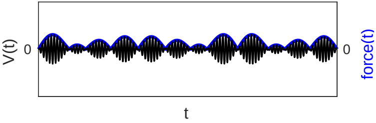

Plasma actuator

- 2 copper electrodes separated by a dielectric material (Kapton tape)
- Plasma arch between the two electrodes ⇒ force on the flow

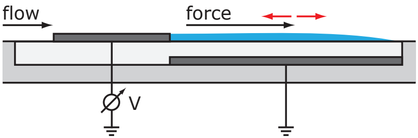

- Driven by the compensator via $u(t) \rightarrow V(t)$

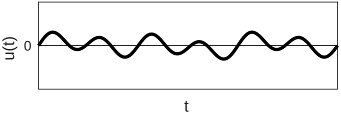

- Force in one direction only: offset + control signal

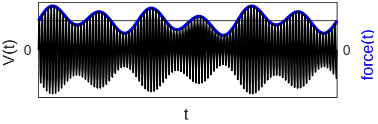

Plasma actuator

- 2 copper electrodes separated by a dielectric material (Kapton tape)
- Plasma arch between the two electrodes $\Rightarrow$ force on the flow

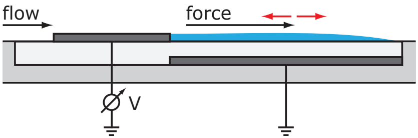

- Driven by the compensator via $u(t) \to V(t)$

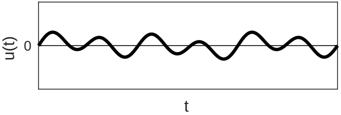

- Force in one direction only: offset + control signal

  Small offset: wave-cancellation (Paper 2, Paper 3)

  Large offset: wave-cancellation + BL stabilisation (Kurz et al., 2013)

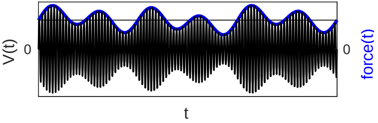

Experimental performance

Performance indicator: $Z = \frac{\sigma_{z,ctr}}{\sigma_{z,unc}}$ (Paper 2)

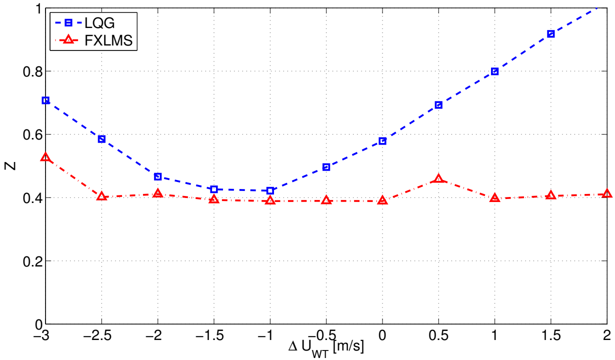

LQG: high dependency on the speed-shift

fxLMS: able to adapt to the modified condition

Delayed-x LMS (dxLMS) algorithm

(Simon et al., 2015, Paper 3)

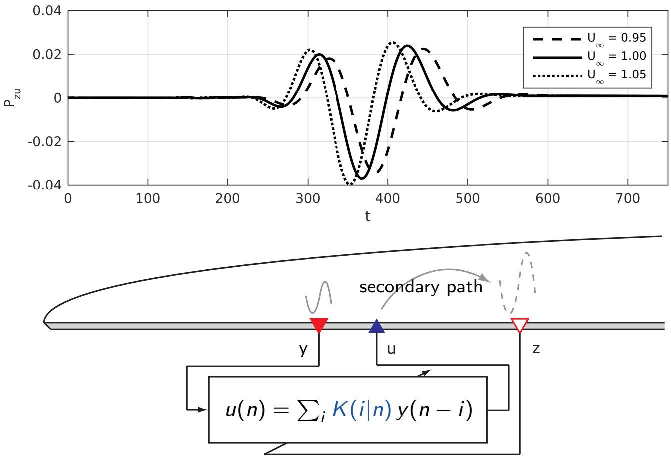

Delayed-x LMS (dxLMS) algorithm

(Simon et al., 2015, Paper 3)

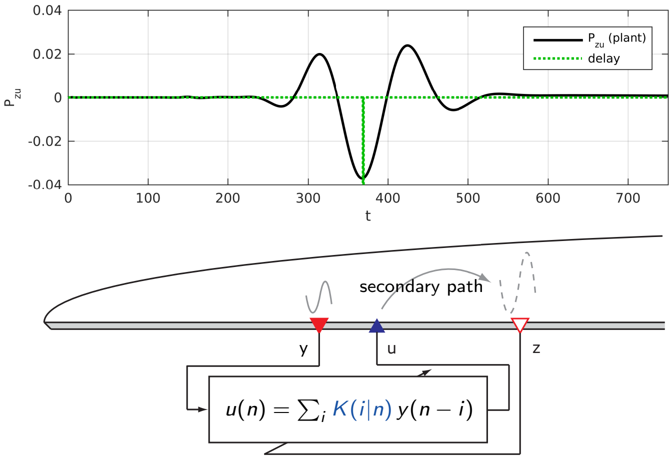

Time-delay identification

Via signal correlation (Paper 3)

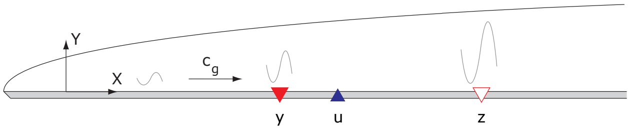

$$\tau_{uz} = \frac{X_z - X_u}{c_g}$$

Time-delay identification

Via signal correlation (Paper 3)

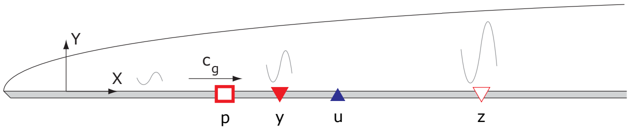

$$c_g \approx \frac{X_y - X_p}{\tau_{py}} \quad \blacktriangleright \quad \tau_{uz} = \frac{X_z - X_u}{c_g}$$

Time-delay identification

Via signal correlation (Paper 3)

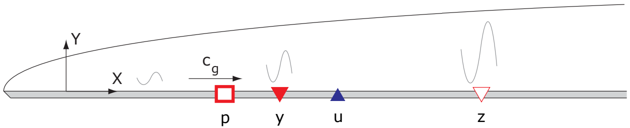

$$c_g \approx \frac{X_y - X_p}{\tau_{py}} \quad \blacktriangleright \quad \tau_{uz} = \frac{X_z - X_u}{c_g} = \frac{X_z - X_u}{X_y - X_p}\,\tau_{py}$$

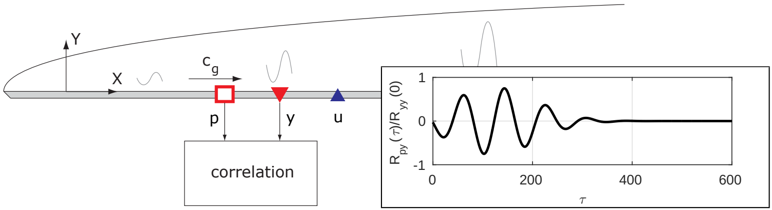

$$c_g \approx \frac{X_y - X_p}{\tau_{py}} \quad \blacktriangleright \quad \tau_{uz} = \frac{X_z - X_u}{c_g} = \frac{X_z - X_u}{X_y - X_p}\,\tau_{py}$$

Time-delay identification

Via signal correlation (Paper 3)

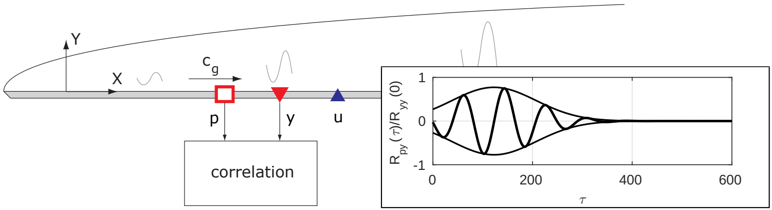

$$c_g \approx \frac{X_y - X_p}{\tau_{py}} \quad \blacktriangleright \quad \tau_{uz} = \frac{X_z - X_u}{c_g} = \frac{X_z - X_u}{X_y - X_p}\,\tau_{py}$$

Time-delay identification

Via signal correlation (Paper 3)

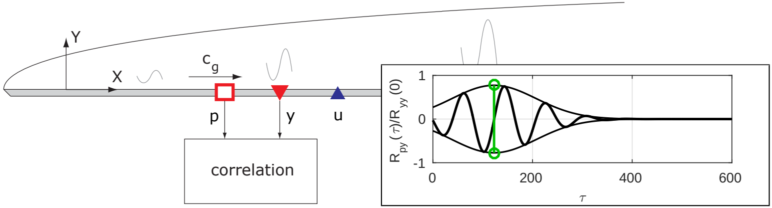

$$c_g \approx \frac{X_y - X_p}{\tau_{py}} \quad \blacktriangleright \quad \tau_{uz} = \frac{X_z - X_u}{c_g} = \frac{X_z - X_u}{X_y - X_p}\,\tau_{py}$$

Time-delay identification

Via signal correlation (Paper 3)

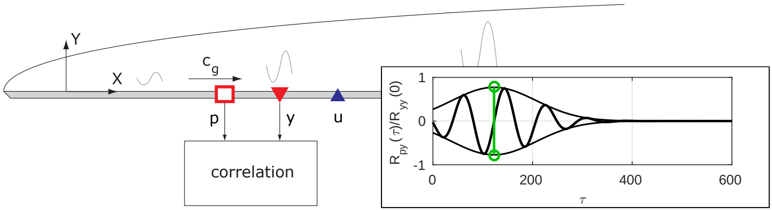

$$c_g \approx \frac{X_y - X_p}{\tau_{py}} \quad \blacktriangleright \quad \tau_{uz} = \frac{X_z - X_u}{c_g} = \frac{X_z - X_u}{X_y - X_p}\,\tau_{py}$$

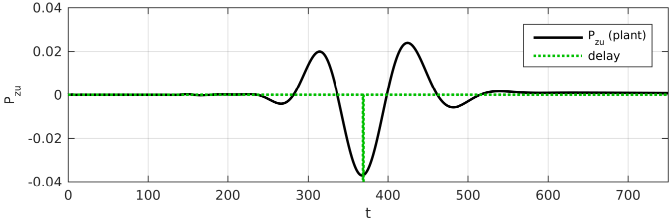

Performace by dxLMS

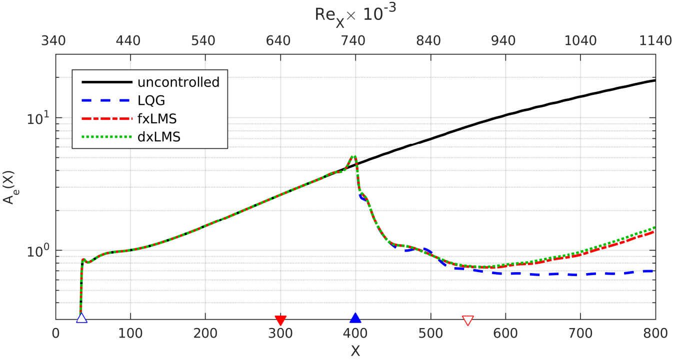

Performace by dxLMS

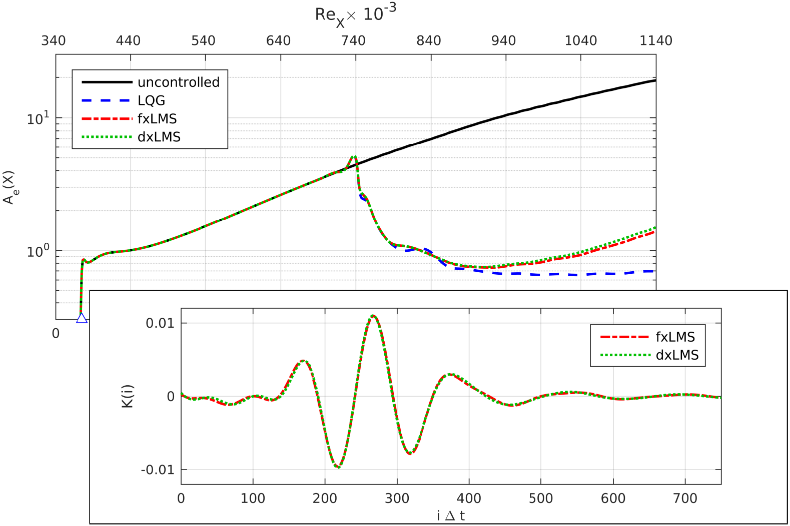

In-flight experiments

Motor-glider Grob G109 @ TU Darmstadt (Paper 3)

In-flight experiments

Motor-glider Grob G109 @ TU Darmstadt (Paper 3)

In-flight experiments

Motor-glider Grob G109 @ TU Darmstadt (Paper 3)

In-flight experiments

Motor-glider Grob G109 @ TU Darmstadt (Paper 3)

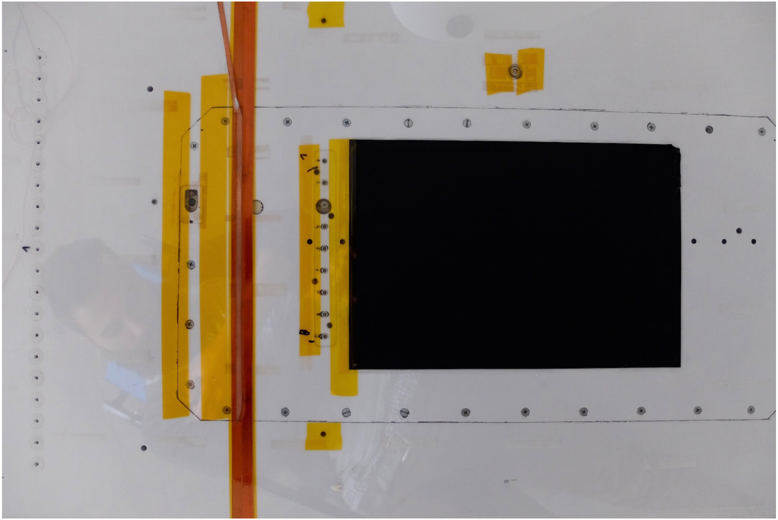

In-flight experiments

Motor-glider Grob G109 @ TU Darmstadt (Paper 3)

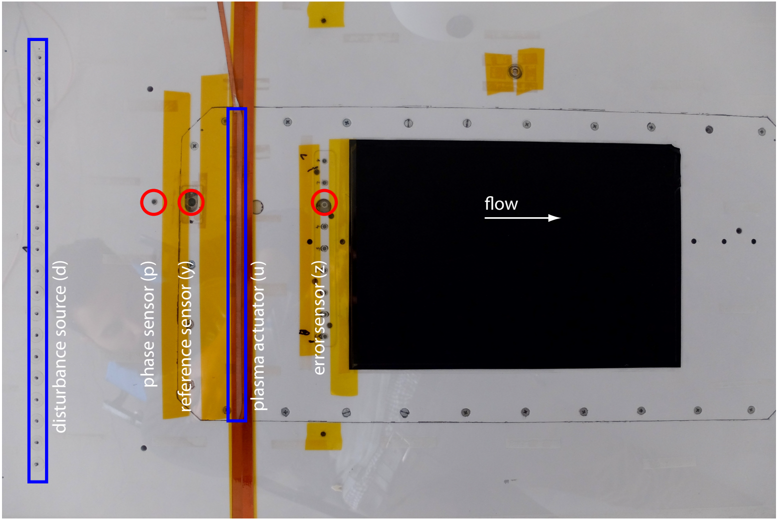

In-flight experiments

Motor-glider Grob G109 @ TU Darmstadt (Paper 3)

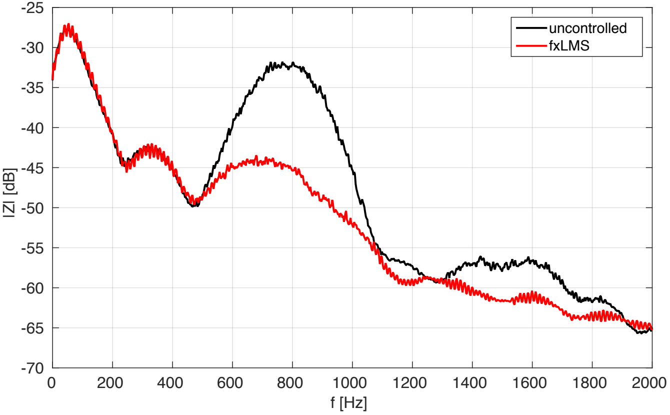

In-flight experiments

Motor-glider Grob G109 @ TU Darmstadt (Paper 3)

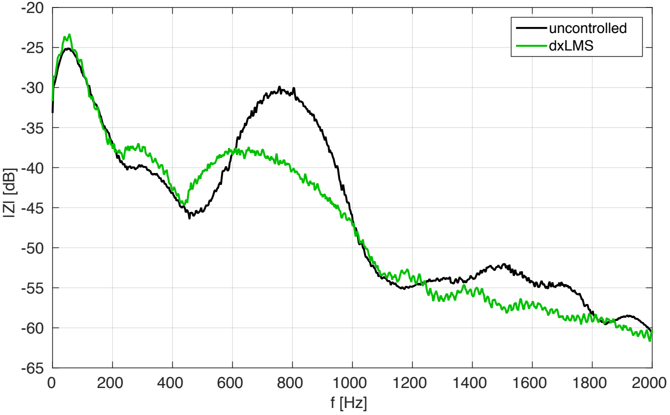

Outline

Control of boundary-layer instabilities
- A linear model of the flow
- Control algorithms
- A self-tuning compensator

Transition delay
- A 3D compensator
- Performance and limitations
- Energy budget

Conclusions and Outlook

From 2D to 3D disturbances

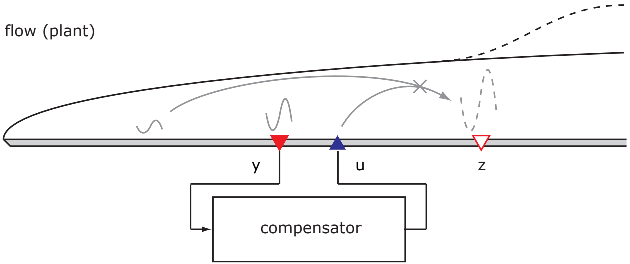

From 2D to 3D disturbances

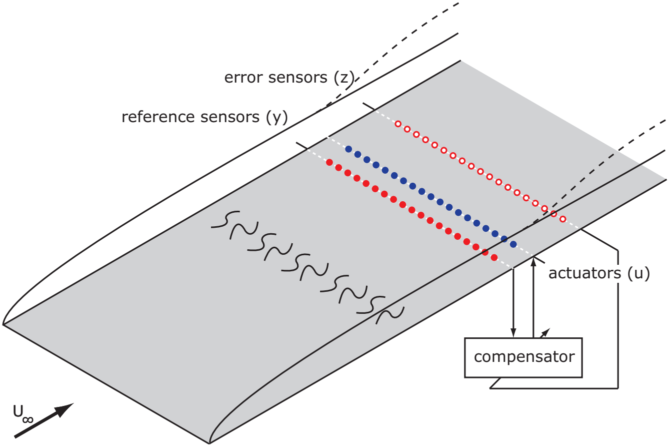

A 3D compensator

Multi-Input Multi-Output (MIMO) (Fabbiane et al., 2015, Paper 5)

$$u_l(n) = \sum_i K_{lm}(i)\, y_m \ (n-i)$$

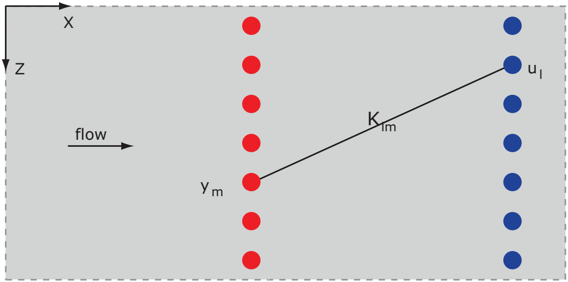

A 3D compensator

Multi-Input Multi-Output (MIMO) (Fabbiane et al., 2015, Paper 5)

$$u_l(n) = \sum_m \sum_i K_{lm}(i)\, y_m \quad (n - i)$$

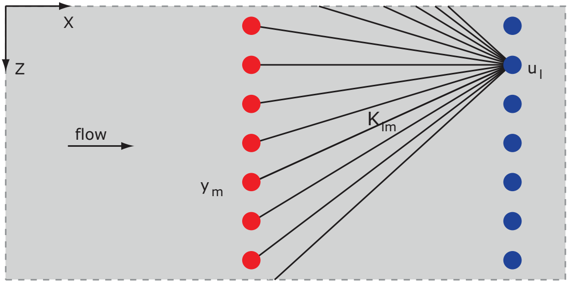

A 3D compensator

Multi-Input Multi-Output (MIMO) (Fabbiane et al., 2015, Paper 5)

$$u_l(n) = \sum_m \sum_i K_{lm}(i)\, y_m \quad (n-i) \quad \forall l$$

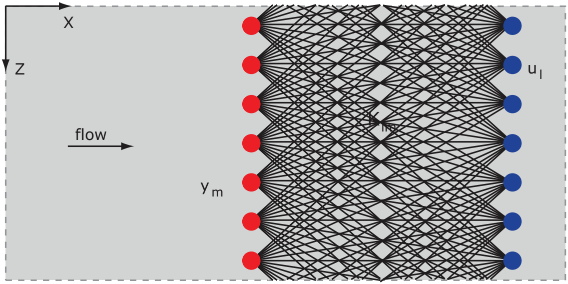

A 3D compensator

Multi-Input Multi-Output (MIMO) (Fabbiane et al., 2015, Paper 5)

$$u_l(n) = \sum_m \sum_i K_m(i)\, y_{m+l}(n-i) \quad \forall l$$

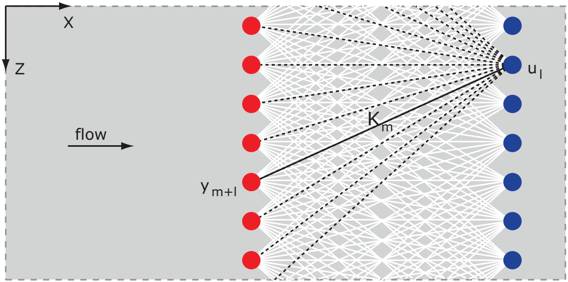

Spanwise homogeneous compensator.

MIMO fxLMS algorithm

(Fabbiane et al., 2015, Paper 5)

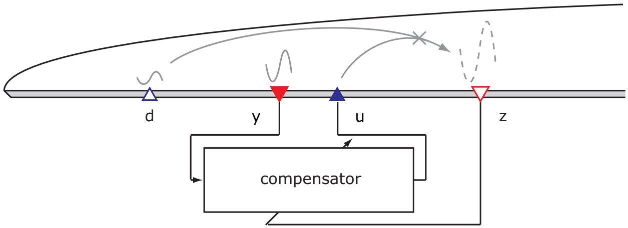

Minimise a measurable cost function

$$\min_{K_m} \left(\sum_l z_l^2(n) \right)$$

via a steepest-descent algorithm:

$$\boxed{K_m(i|n+1) = K_m(i|n) - \mu\, \lambda_m(i|n)}$$

where $\lambda_m(i|n) = \frac{\partial}{\partial K_m(i)} \left(\sum_l z_l^2(n)\right) = 2\, \sum_l\, z_l(n)\, \sum_r \sum_j P_{zu,r}(j)\, y_{r+m+l}(n-j-i)$.

Transition delay

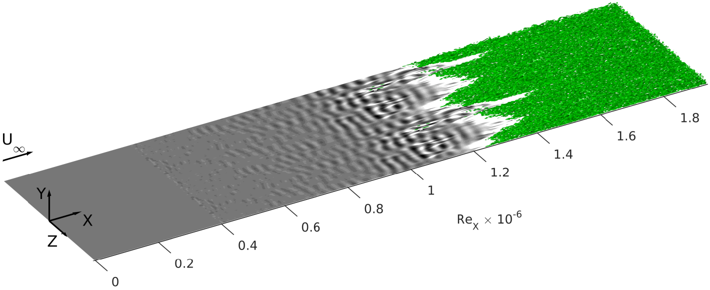

Transition delay

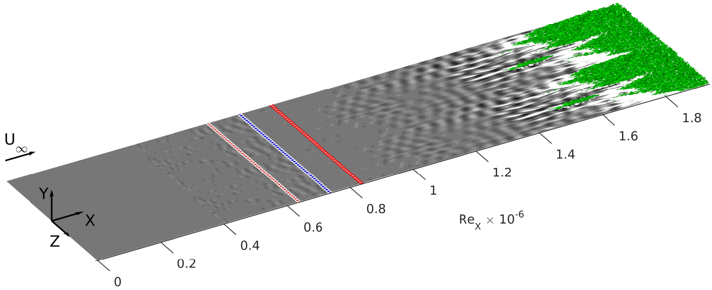

Transition delay

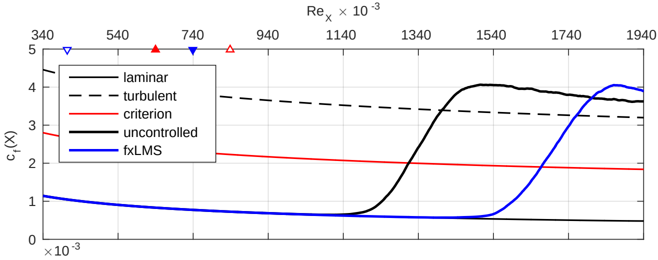

Transition delay

$$A^2(X) = \max_Y \left\langle \left(\frac{u'}{U}\right)^2 \right\rangle_{Z,t} \text{ @ } X = 100$$

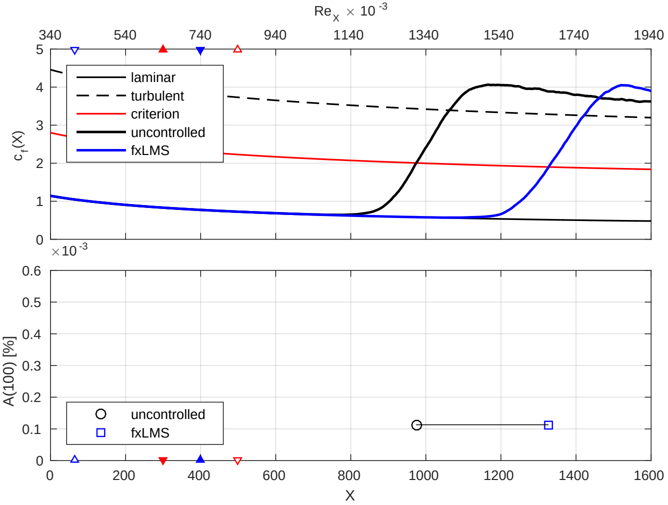

Transition delay

$$A^2(X) = \max_Y \left\langle \left(\frac{u'}{U} \right)^2 \right\rangle_{Z,t} \quad @\ X = 100$$

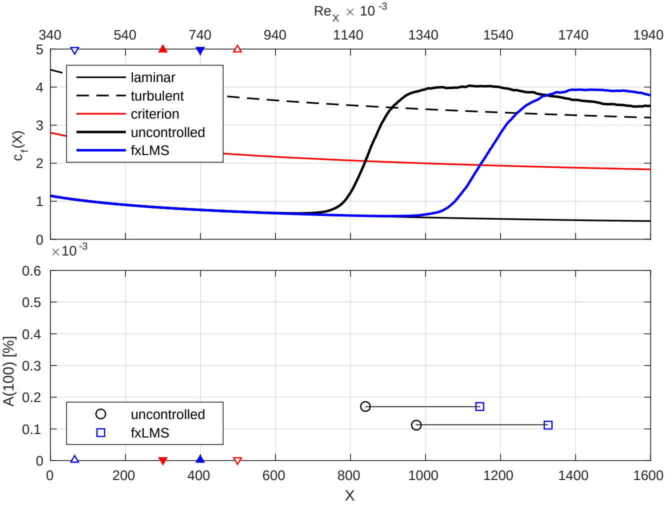

Transition delay

$$A^2(X) = \max_Y \left\langle \left(\frac{u'}{U}\right)^2 \right\rangle_{Z,t} \text{ @ } X = 100$$

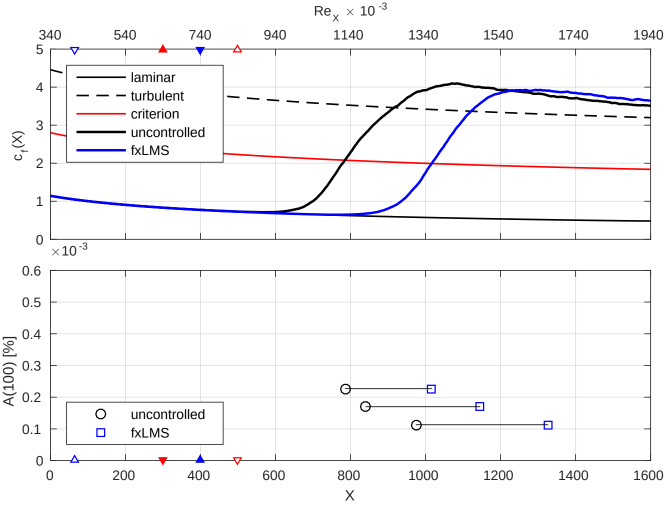

Transition delay

$$A^2(X) = \max_Y \left\langle \left(\frac{u'}{U}\right)^2 \right\rangle_{Z,t} \text{ @ } X = 100$$

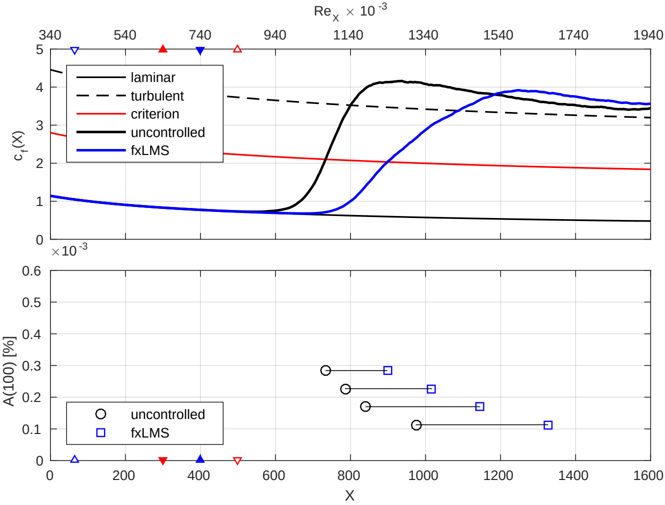

Transition delay

$$A^2(X) = \max_Y \left\langle \left(\frac{u'}{U} \right)^2 \right\rangle_{Z,t} \quad @ \; X = 100$$

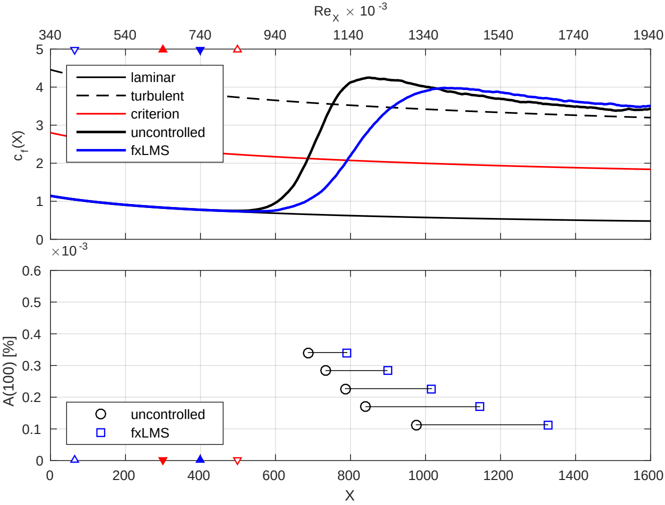

Transition delay

$$A^2(X) = \max_Y \left\langle \left(\frac{u'}{U}\right)^2 \right\rangle_{Z,t} \quad @ \; X = 100$$

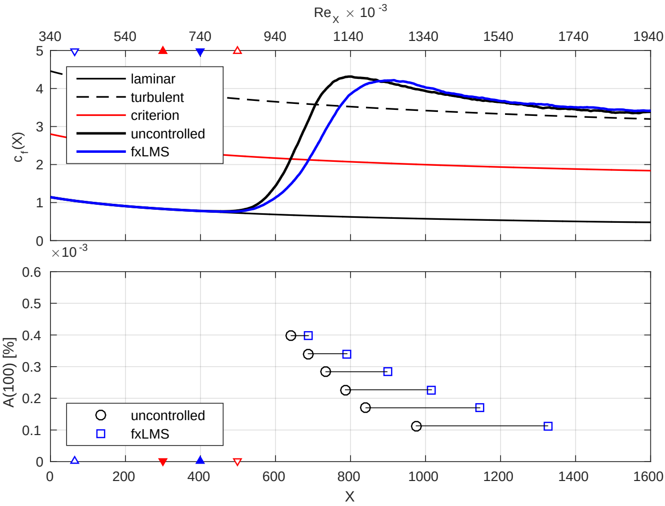

Transition delay

$$A^2(X) = \max_Y \left\langle \left(\frac{u'}{U}\right)^2 \right\rangle_{Z,t} \text{ @ } X = 100$$

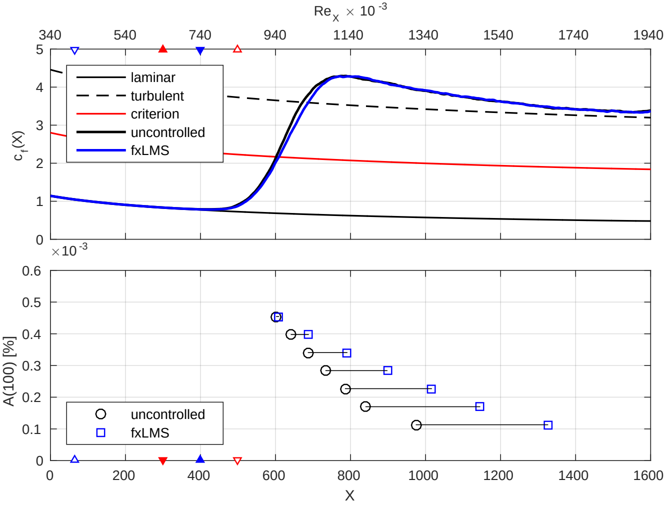

Transition delay

$$A^2(X) = \max_Y \left\langle \left(\frac{u'}{U} \right)^2 \right\rangle_{Z,t} \quad @ \ X = 100$$

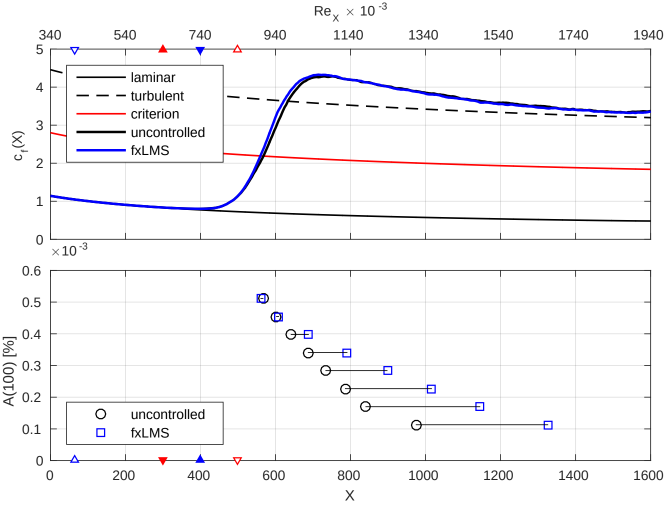

Transition delay

$$A^2(X) = \max_Y \left\langle \left(\frac{u'}{U}\right)^2 \right\rangle_{Z,t} \text{ @ } X = 100$$

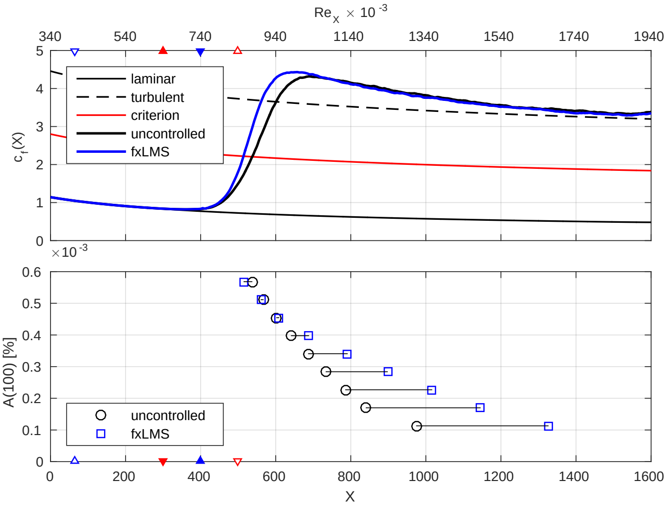

The non-linear challenge

Wall shear-stress spectra at $X = 500$

uncontrolled

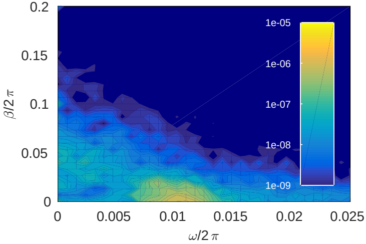

Linear: $A(400) = 0.19\%$

FLOW

The non-linear challenge

Wall shear-stress spectra at $X = 500$

uncontrolled

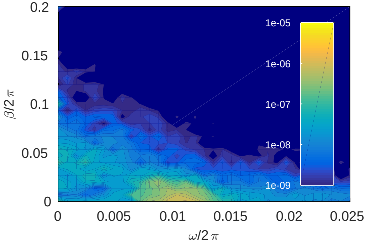

controlled

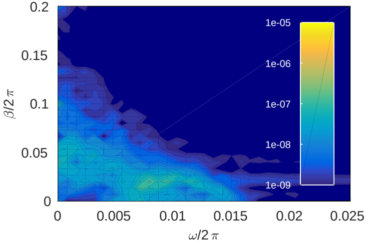

Linear: $A(400) = 0.19\%$

The non-linear challenge

Wall shear-stress spectra at $X = 500$

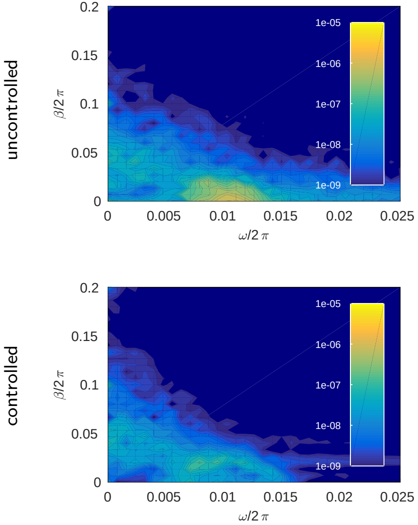

Linear: $A(400) = 0.19\%$ Weakly non-linear: $A(400) = 0.55\%$

The non-linear challenge

Wall shear-stress spectra at $X = 500$

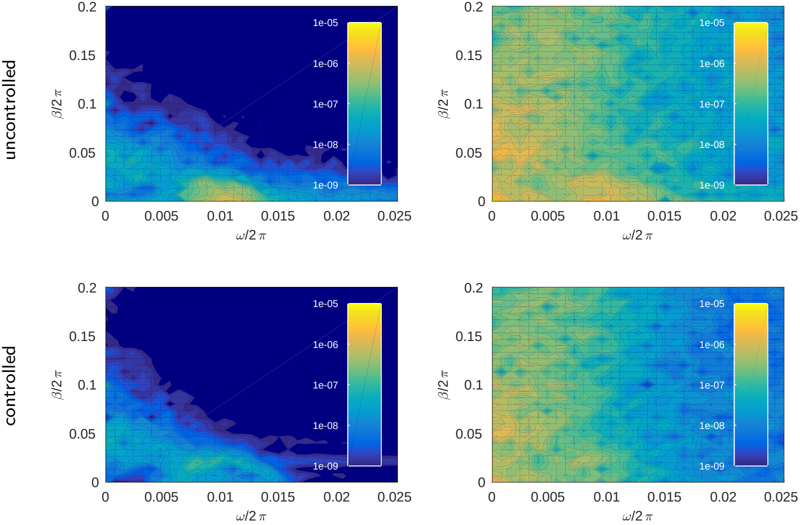

Linear: $A(400) = 0.19\%$

Non-linear: $A(400) = 1.33\%$

The non-linear challenge

Wall shear-stress spectra at $X = 500$

uncontrolled

controlled

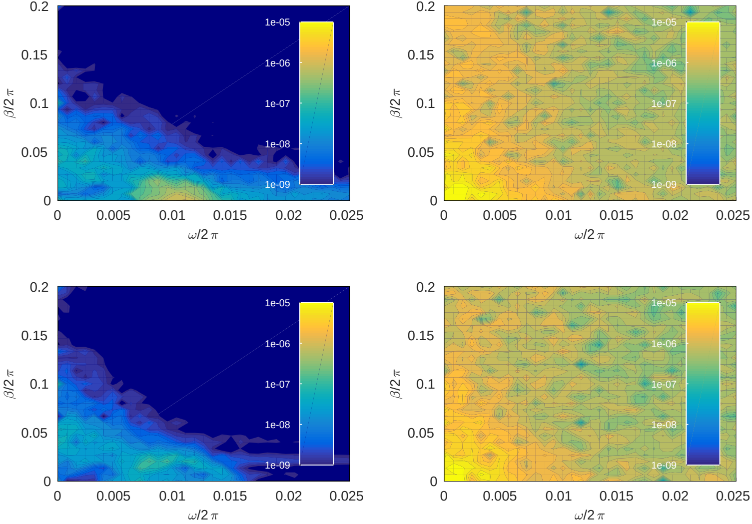

Linear: $A(400) = 0.19\%$

Transitional: $A(400) = 2.97\%$

The non-linear challenge

Compensator performance

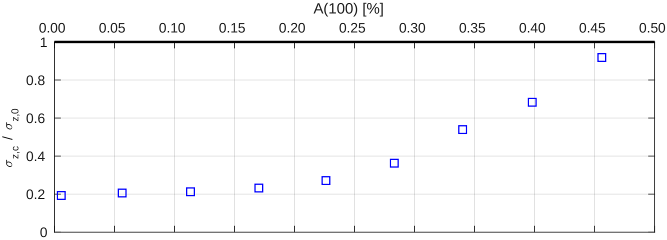

The non-linear challenge

Compensator performance

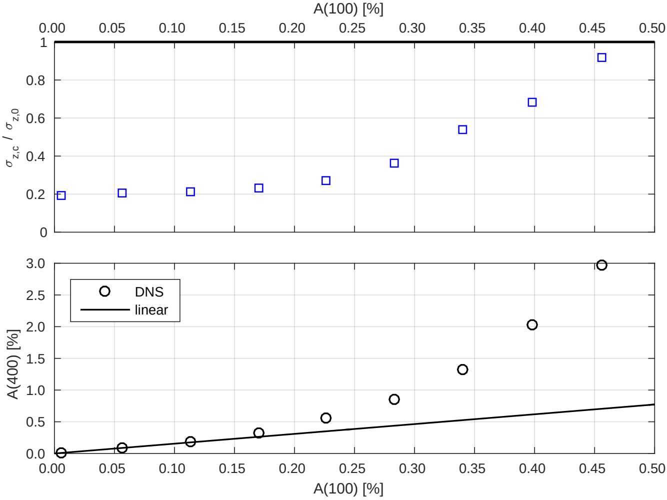

The non-linear challenge

Compensator performance

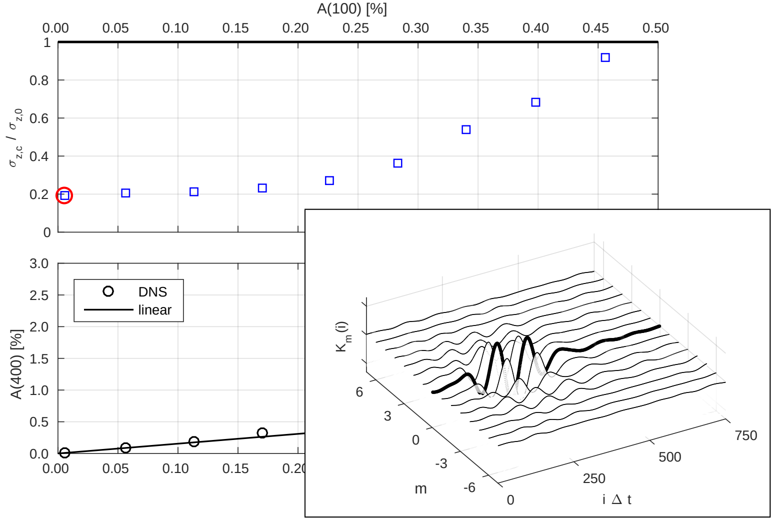

The non-linear challenge

Compensator performance

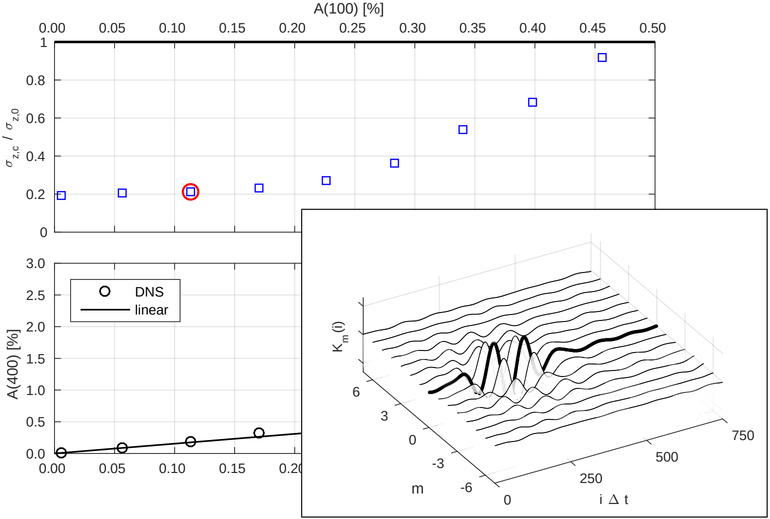

The non-linear challenge

Compensator performance

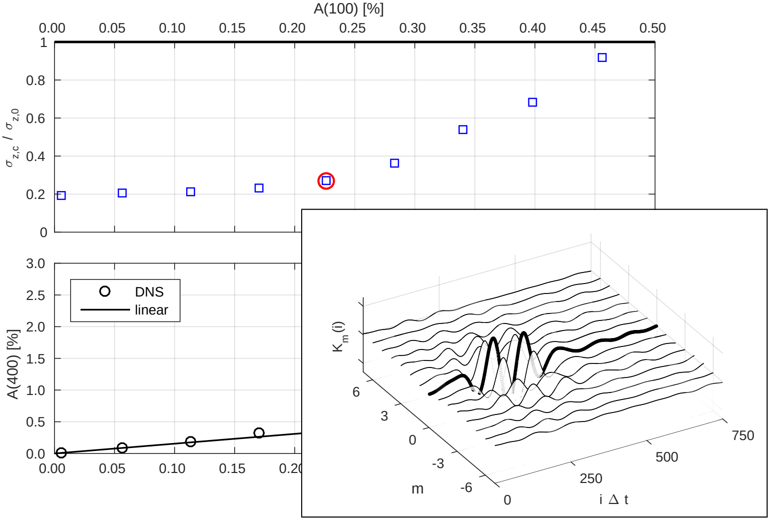

The non-linear challenge

Compensator performance

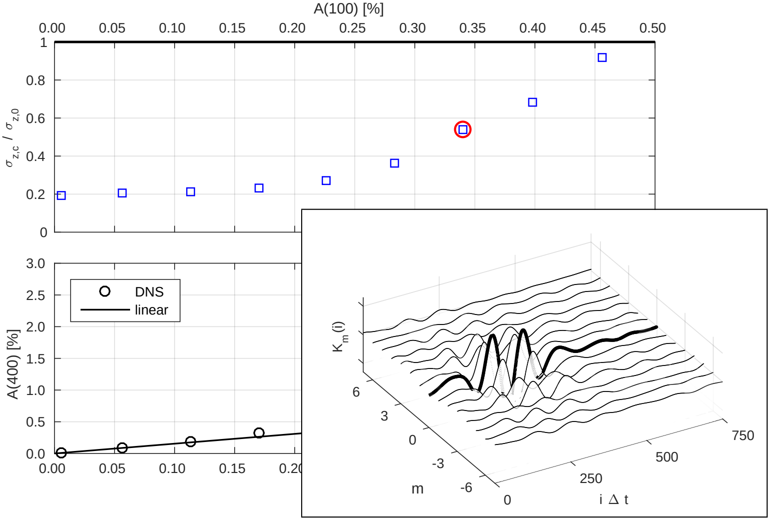

The non-linear challenge

Compensator performance

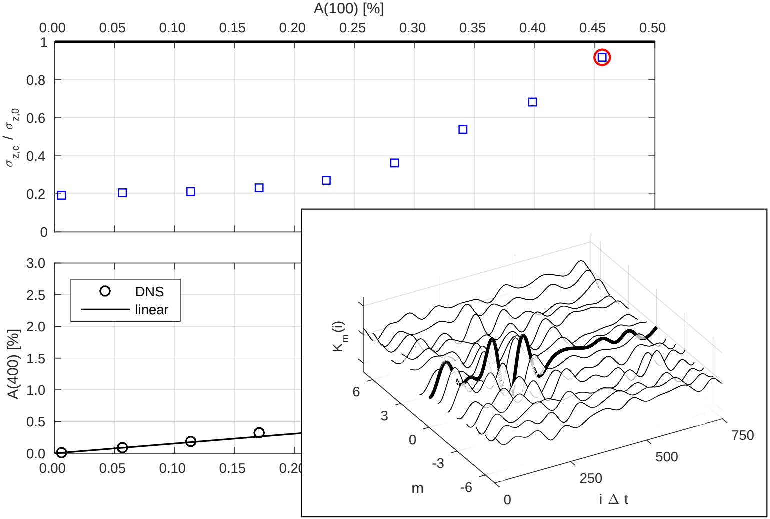

Energy budget

Saved power ($P_s = U_\infty \, \Delta D$)

Drag reduction: $$\frac{\Delta D}{L_Z} = \int_0^{L_X} \left\langle \tau_{w,0} - \tau_{w,c} \right\rangle_{Z,t} \, dX$$

Energy budget

Saved power ($P_s = U_\infty \, \Delta D$)

Drag reduction: $$\frac{\Delta D}{L_Z} = \int_0^{L_X} \langle \tau_{w,0} - \tau_{w,c} \rangle_{Z,t} \; dX$$

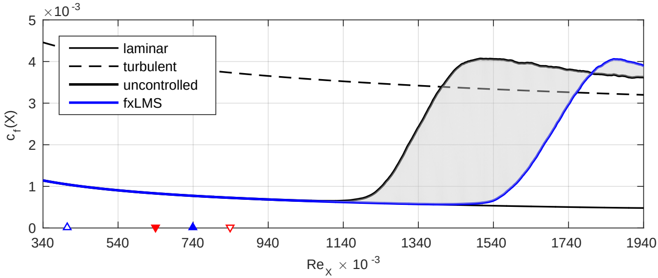

Energy budget

Saved power ($P_s = U_\infty \, \Delta D$)

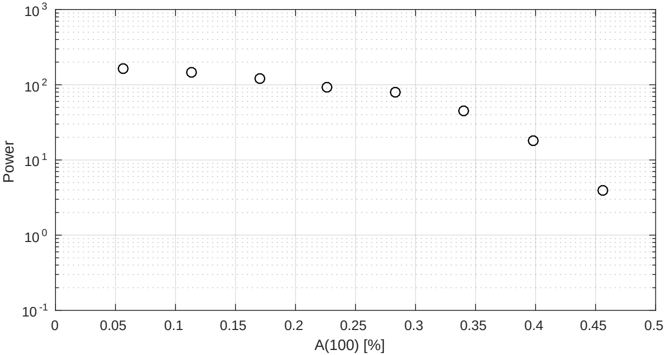

Energy budget

Saved power ($P_s = U_\infty \, \Delta D$) vs. control power ($P_c$, Kriegseis et al., 2011, 2013)

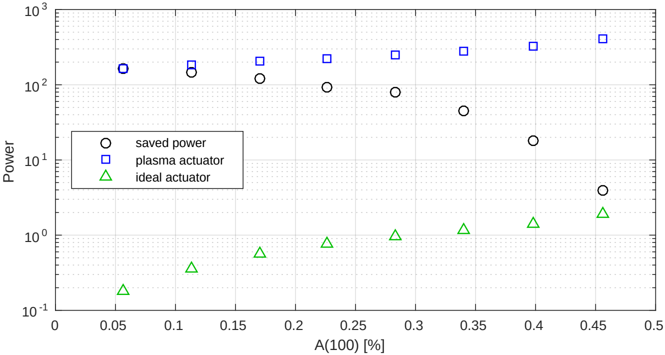

Energy budget

Saved power ($P_s = U_\infty \, \Delta D$) vs. control power ($P_c$, Kriegseis et al., 2011, 2013)

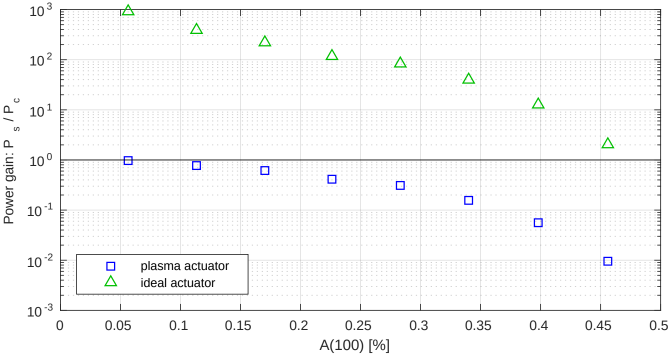

Energy budget

Saved power ($P_s = U_\infty \, \Delta D$) vs. control power ($P_c$, Kriegseis et al., 2011, 2013)

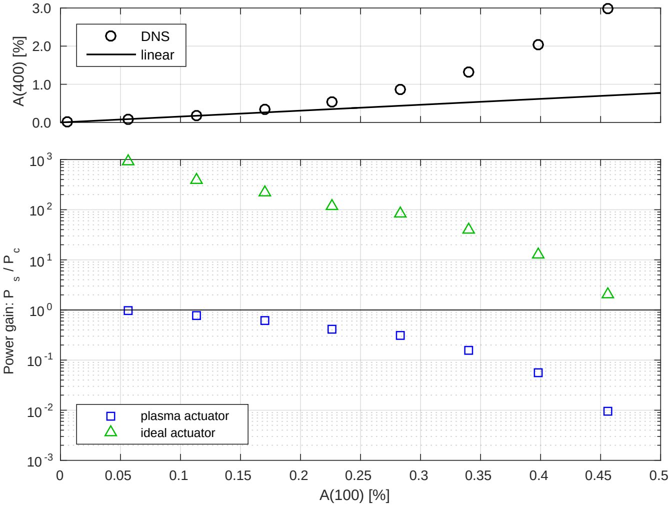

Outline

Control of boundary-layer instabilities

A linear model of the flow

Control algorithms

A self-tuning compensator

Transition delay

A 3D compensator

Performance and limitations

Energy budget

Conclusions and Outlook

Conclusions

- Model-based control may present robustness issues:
  - robustness can be recovered via adaptive algorithms.

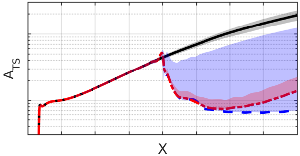

Conclusions

- Model-based control may present robustness issues:
  - robustness can be recovered via adaptive algorithms.

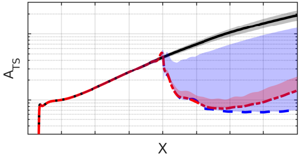

- Transition is effectively and efficiently delayed.

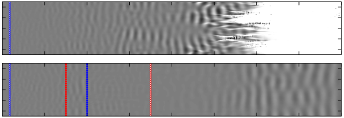

Conclusions

- Model-based control may present robustness issues:
  - robustness can be recovered via adaptive algorithms.

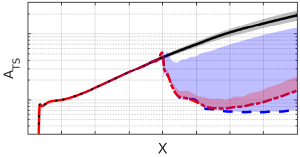

- Transition is effectively and efficiently delayed.

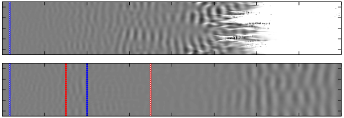

- In-flight experiments by using plasma actuators.

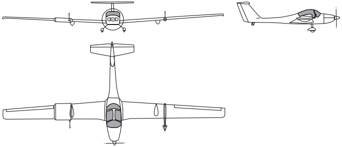

Outlook

Disturbance: control of different disturbances than TS waves.

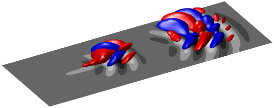

Outlook

Disturbance: control of different disturbances than TS waves.

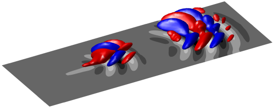

Actuator: improve energy efficiency.

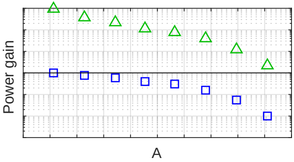

Outlook

Disturbance: control of different disturbances than TS waves.

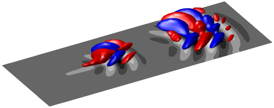

Actuator: improve energy efficiency.

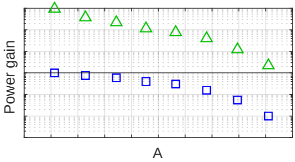

Algorithm: overcome the limitation given by non-linearities.

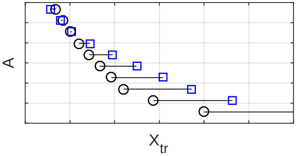

Outlook

Disturbance: control of different disturbances than TS waves.

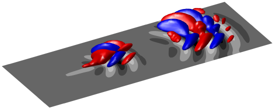

Actuator: improve energy efficiency.

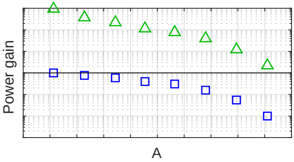

Algorithm: overcome the limitation given by non-linearities.

- Machine learning?

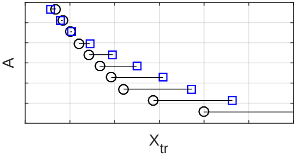

PhD defense

Stockholm – June 13th, 2016

Respondent
Nicolò Fabbiane

Opponent
Dr. Denis Sipp, ONERA DAFE, France

Committee
Dr. Ati Sharma, Univ. of Southampton, UK
Dr. Taraneh Sayadi, RWTH Aachen, Germany
Prof. Håkan Hjalmarsson, KTH Aut. Control

Chairman
Dr. Ardeshir Hanifi, FOI/KTH Mechanics

Main advisor
Prof. Dan S. Henningson, KTH Mechanics

Co-advisor
Dr. Shervin Bagheri, KTH Mechanics

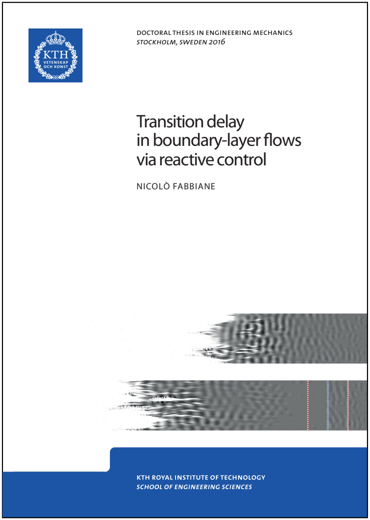
DOCTORAL THESIS IN ENGINEERING MECHANICS
STOCKHOLM, SWEDEN 2016

Transition delay in boundary-layer flows via reactive control

NICOLÒ FABBIANE

KTH ROYAL INSTITUTE OF TECHNOLOGY
SCHOOL OF ENGINEERING SCIENCES

Public defense:

1. Presentation by the respondent (ca 40 min).
2. The opponent discusses the thesis with the respondent.
3. The members of the grading committee discuss the thesis with the respondent.
4. The audience is allowed and invited to ask questions.

Public defense:

1. Presentation by the respondent (ca 40 min).
2. The opponent discusses the thesis with the respondent.
3. The members of the grading committee discuss the thesis with the respondent.
4. The audience is allowed and invited to ask questions.

The procedure continues as follows:

1. The grading committee will deliberate behind locked doors and make a decision.
2. The decision will be announced by the committee at Mechanics department, Osquars Backe 18, 6th floor.
3. Lunch will be served for all the involved people, including registered participating audience.

References

Bagheri, S., Brandt, L., and Henningson, D. S. (2009). Input–output analysis, model reduction and control of the flat-plate boundary layer. *J. Fluid Mech.*, 620(1):263–298.

Barbagallo, A., Sipp, D., and Schmid, P. J. (2009). Closed-loop control of an open cavity flow using reduced order models. *J. Fluid Mech.*, 641:1–50.

Bewley, T. R. and Liu, S. (1998). Optimal and Robust Control and Estimation of Linear Paths to Transition. *J. Fluid Mech.*, 365:305–349.

Brunton, S. L. and Noack, B. R. (2015). Closed-loop turbulence control: Progress and challenges. *Applied Mechanics Reviews*, 67(5):AMR–14–1091.

Chevalier, M., Schlatter, P., Lundbladh, A., and Henningson, D. S. (2007). A pseudo-spectral solver for incompressible boundary layer flows. Technical Report TRITA-MEK 2007:07, KTH Mechanics, Stockholm, Sweden.

Fabbiane, N., Bagheri, S., and Henningson, D. S. (2015). Adaptive control of finite-amplitude 3D disturbances in 2D boundary-layer flows. In *Proceedings of TSFP-9*, Melbourne.

Juang, J.-N. and Pappa, R. S. (1985). An eigensystem realization algorithm for modal parameter identification and model reduction. *J. Guid., Con. Dyn.*, 8(5):620–627.

Juillet, F., McKeon, B. J., and Schmid, P. J. (2014). Experimental Control of Natural Perturbations in Channel Flow. *J. Fluid Mech.*, 752:296–309.

Kotsonis, M., Shukla, R. K., and Pröbsting, S. (2015). Control of Natural Tollmien-Schlichting Waves using Dielectric Barrier Discharge Plasma Actuators. *Intl J. of Flow Control*, 7(1-2):37–54.

Kriegseis, J., Möller, B., Grundmann, S., and Tropea, C. (2011). Capacitance and power consumption quantification of dielectric barrier discharge (DBD) plasma actuators. *Journal of Electrostatics*, 69(4):302–312.

Kriegseis, J., Schwarz, C., Tropea, C., and Grundmann, S. (2013). Velocity-Information-Based Force-Term Estimation of Dielectric-Barrier Discharge Plasma Actuators. *J. Phys. D*, 46(5):055202.

Kurz, A., Goldin, N., King, R., Tropea, C. D., and Grundmann, S. (2013). Hybrid Transition Control Approach for Plasma Actuators. *Exp. Fluids*, 54(11):1–4.

Li, Y. and Gaster, M. (2006). Active Control of Boundary-Layer Instabilities. *J. Fluid Mech.*, 550:185–205.

Ma, Z., Ahuja, S., and Rowley, C. W. (2011). Reduced-order models for control of fluids using the eigensystem realization algorithm. *Theoretical and Computational Fluid Dynamics*, 25(1-4):233–247.

Morkovin, M., Reshotko, E., and Herbert, T. (1994). Transition in open flow systems-a reassessment. *Bull. Am. Phys. Soc*, 39(9):1882.

Semeraro, O., Bagheri, S., Brandt, L., and Henningson, D. S. (2013). Transition delay in a boundary layer flow using active control. *J. Fluid Mech.*, 731(9):288–311.

Sharma, A. S., Morrison, J. F., McKeon, B. J., Limebeer, D. J. N., Koberg, W. H., and Sherwin, S. J. (2011). Relaminarisation of $Re_\tau = 100$ channel flow with globally stabilising linear feedback control. *Physics of Fluids*, 23(12).

Simon, B., Nemitz, T., Rohlfing, J., Fischer, F., Mayer, D., and Grundmann, S. (2015). Active flow control of laminar boundary layers for variable flow conditions. *Intl J. Heat and Fluid Flow*, 56:344–354.

Snyder, S. D. and Hansen, C. H. (1994). The effect of transfer function estimation errors on the filtered-x LMS algorithm. *IEEE Transactions on Signal Processing*, 42(4):950–953.

). an
Intl J. Heat and

Noise-amplifier vs. oscillator

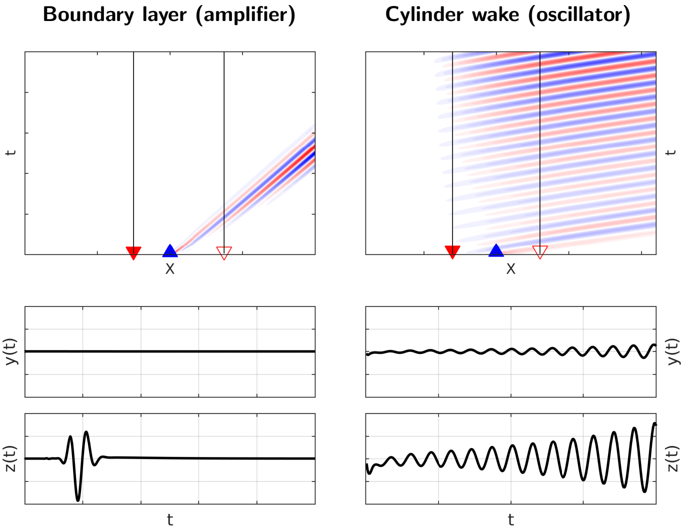

Plant response

Noise response by the disturbance d

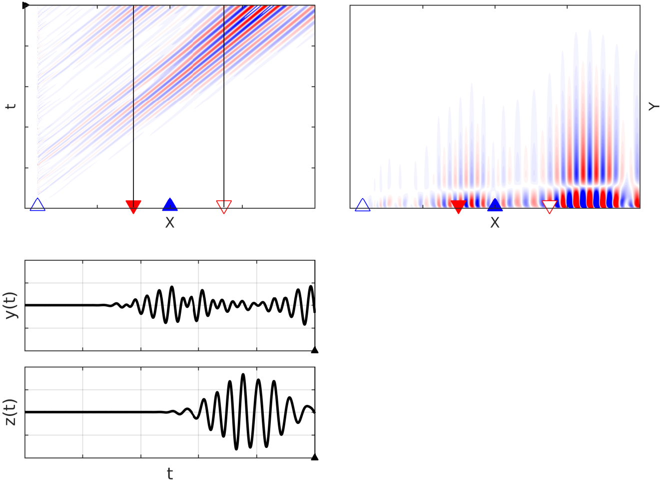

Plant response

Noise response by the disturbance d

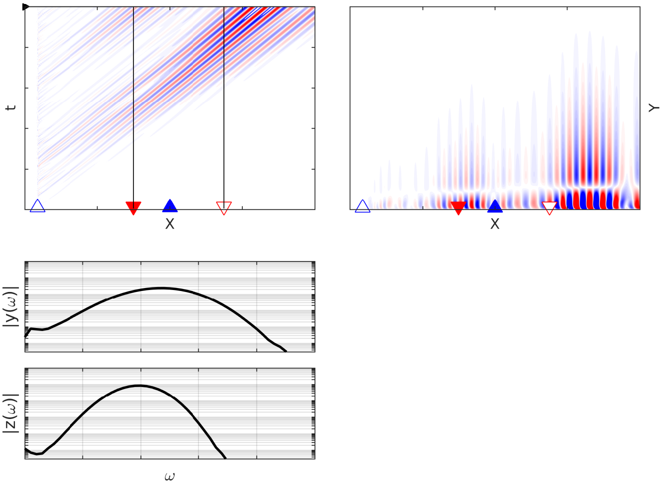

Plant response

Noise response by the disturbance d

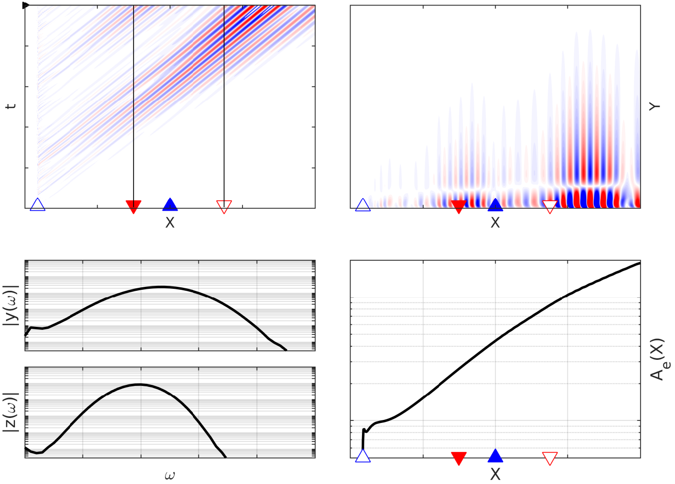

Model-reduction

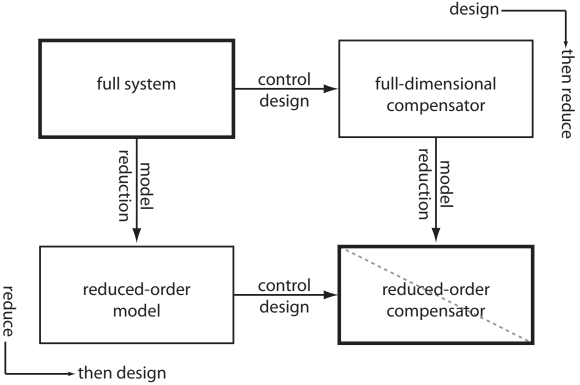

Model-reduction

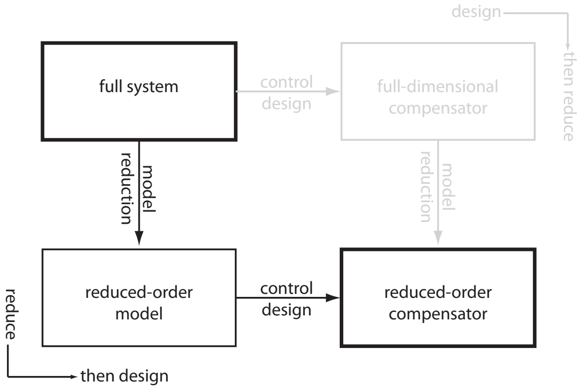

Model-reduction

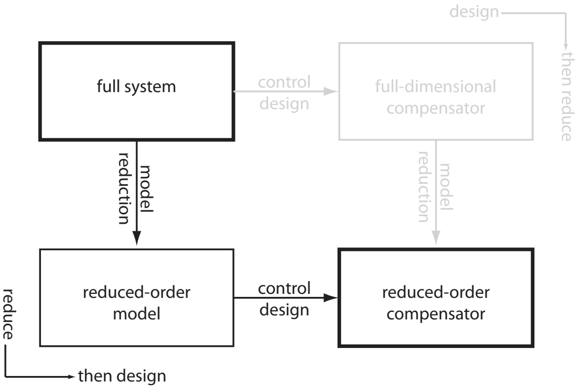

In this work, Eigensystem realisation algorithm (ERA) is used (Juang and Pappa, 1985).

- Equivalent to a Galerkin projection over BPOD modes (Ma et al., 2011).

Stability limit for fxLMS algorithm

Snyder and Hansen (1994)

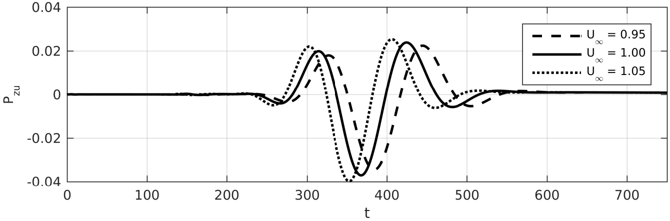

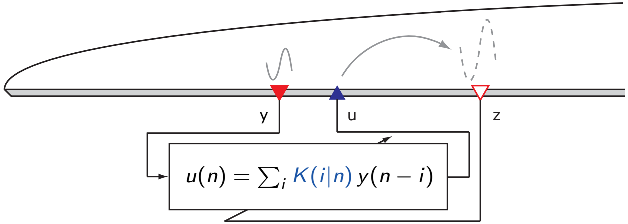

Stability limit for fxLMS algorithm

Snyder and Hansen (1994)

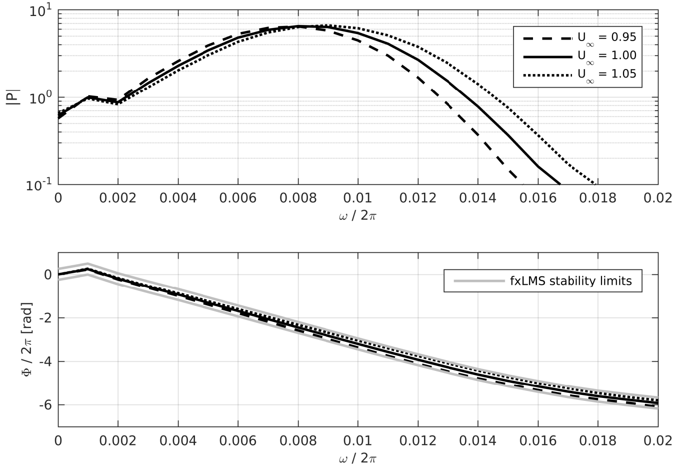

Stability limit for fxLMS algorithm

Snyder and Hansen (1994)

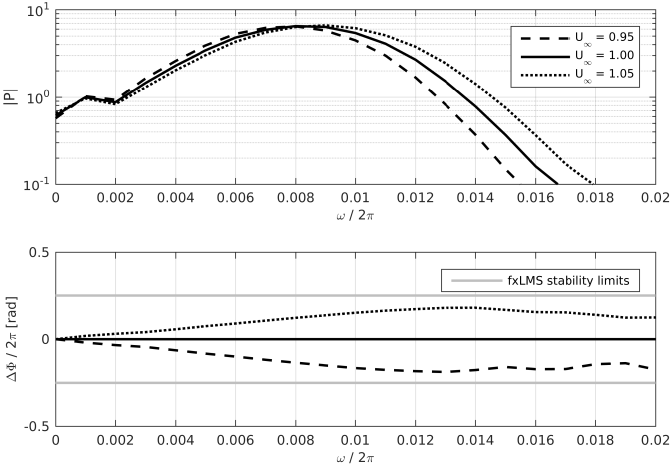

Stability limit for fxLMS algorithm

Snyder and Hansen (1994)

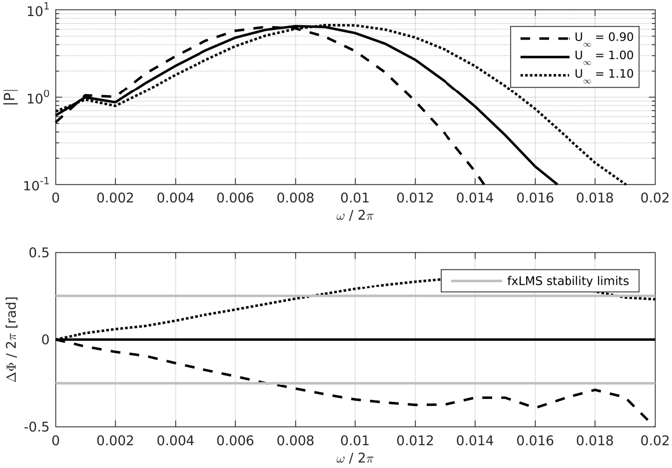

Stability limit for fxLMS algorithm

Snyder and Hansen (1994)

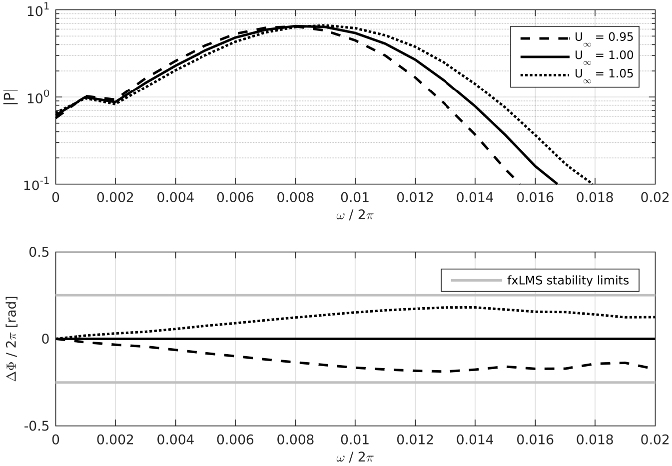

Time-delay identification

Via signal correlation (Simon et al., 2015, Paper 3)

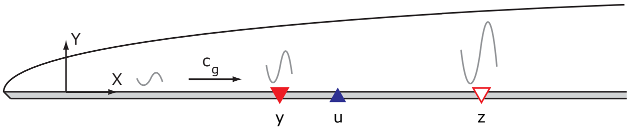

Time-delay identification

Via signal correlation (Simon et al., 2015, Paper 3)

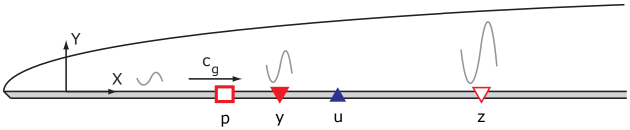

Time-delay identification

Via signal correlation (Simon et al., 2015, Paper 3)

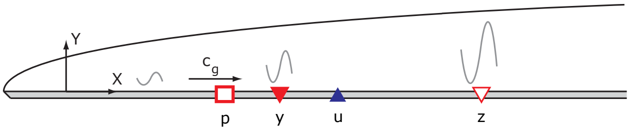

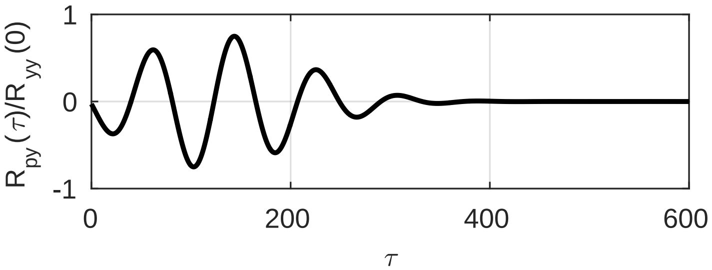

Time-delay identification

Via signal correlation (Simon et al., 2015, Paper 3)

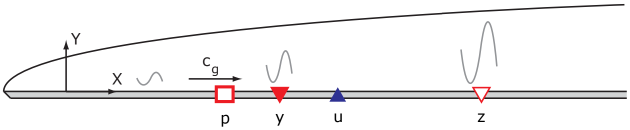

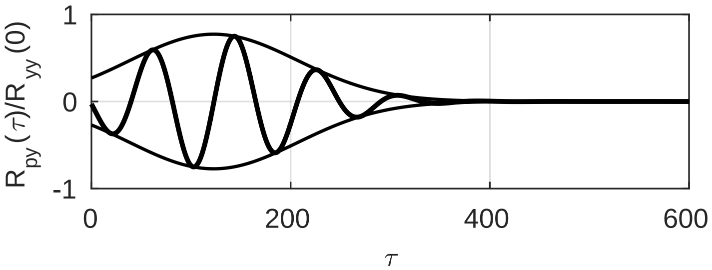

Time-delay identification

Via signal correlation (Simon et al., 2015, Paper 3)

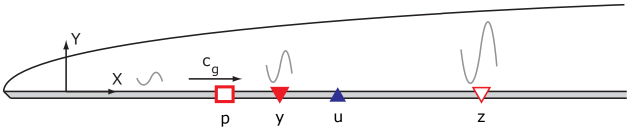

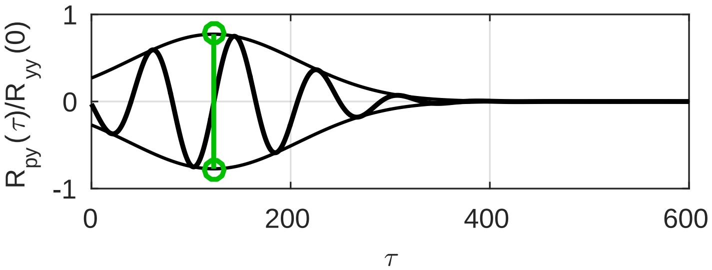

Time-delay identification

Via signal correlation (Simon et al., 2015, Paper 3)

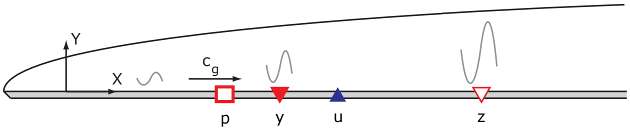

$$c_g \approx \frac{X_y - X_p}{\tau_{py}}$$

Time-delay identification

Via signal correlation (Simon et al., 2015, Paper 3)

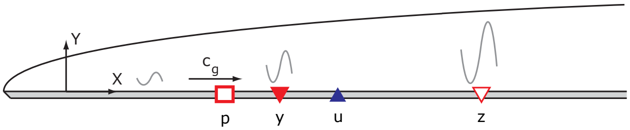

$$c_g \approx \frac{X_y - X_p}{\tau_{py}} \quad \blacktriangleright \quad \tau_{uz} = \frac{X_z - X_u}{c_g}$$

Time-delay identification

Via signal correlation (Simon et al., 2015, Paper 3)

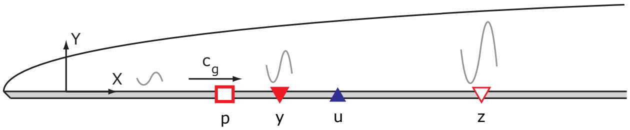

$$c_g \approx \frac{X_y - X_p}{\tau_{py}} \quad \blacktriangleright \quad \tau_{uz} = \frac{X_z - X_u}{c_g} = \frac{X_z - X_u}{X_y - X_p}\,\tau_{py}$$

Time-delay identification

Via signal correlation (Simon et al., 2015, Paper 3)

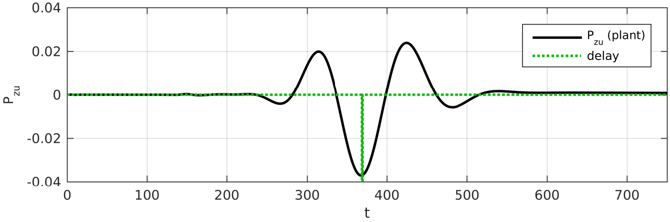

Time-delay identification

Via signal correlation (Simon et al., 2015, Paper 3)